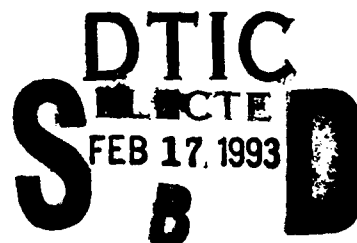AD-A261 730

PL-TR-92-2324

THE DISTANCE DEPENDENCE OF REGIONAL PHASE DISCRIMINANTS

Brian L. N. Kennett

Australian National University
Research School of Earth Sciences
GPO Box 4
Canberra ACT 2601, AUSTRALIA

DTIC
S ELECTE
FEB 17, 1993
B D

9 November 1992

Scientific Report No. 2

PHILLIPS LABORATORY
Directorate of Geophysics
AIR FORCE MATERIEL COMMAND
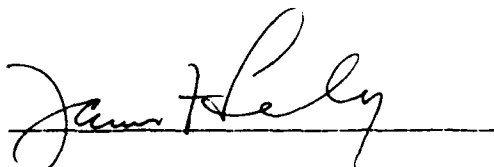HANSCOM AIR FORCE BASE, MA 01731-5000
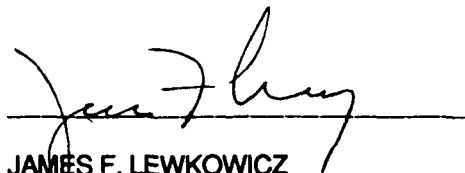
93-04844

93 2 16 054

The views and conclusions contained in this document are those of the authors and should not be interpreted as representing the official policies, either expressed or implied, of the Air Force or the U.S. Government.

This technical report has been reviewed and is approved for publication.

JAMES F. LEWKOWICZ
Contract Manager
Solid Earth Geophysics Branch
Earth Sciences Division

JAMES F. LEWKOWICZ
Branch Chief
Solid Earth Geophysics Branch
Earth Sciencs Division

DONALD H. ECKHARDT, Director
Earth Sciences Division

This document has been reviewed by the ESD Public Affairs Office (PA) and is releasable to the National Technical Information Service (NTIS).

Qualified requestors may obtain additional copies from the Defense Technical Information Center. All others should apply to the National Technical Information Service.

If your address has changed, or if you wish to be removed from the mailing list, or if the addressee is no longer employed by your organization, please notify PL/IMA, Hanscom AFB MA 01731-5000. This will assist us in maintaining a current mailing list.

Do not return copies of this report unless contractual obligations or notices on a specific document requires that it be returned.

REPORT DOCUMENTATION PAGE

1. AGENCY USE ONLY (Leave blank)	2. REPORT DATE	3. REPORT TYPE AND DATES COVERED
	9 November 1992	Scientific #2 (30 Sept 1991–31 Oct 1992)

4. TITLE AND SUBTITLE	5. FUNDING NUMBERS
THE DISTANCE DEPENDENCE OF REGIONAL PHASE DISCRIMINANTS	Grant AFOSR-90-0352 PE 62101F PR 7600 TA 09 WU AO

6. AUTHOR(S)

Brian L.N. Kennett

7. PERFORMING ORGANIZATION NAME(S) AND ADDRESS(ES)

Australian National University
Research School of Earth Sciences
GPO Box 4
CANBERRA ACT 2601
AUSTRALIA

8. PERFORMING ORGANIZATION REPORT NUMBER

9. SPONSORING/MONITORING AGENCY NAME(S) AND ADDRESS(ES)

Phillips Laboratory
Hanscom AFB, MA 01731-5000

Contract Manager: James Lewkowicz/GPEH

10. SPONSORING/MONITORING AGENCY REPORT NUMBER

PL-TR-92-2324

11. SUPPLEMENTARY NOTES

12b. DISTRIBUTION CODE

13. ABSTRACT (Maximum 200 words)

Amplitude ratios of P and S phases recorded at regional distances have been suggested as potential discriminants for the character of seismic sources, because of the differences expected in the radiation patterns of earthquakes and well-contained explosions. The most useful reference phase for P waves beyond 200 km from the source is Pn and for S possible choices are the mantle phase Sn and the crustally guided wave Lg. Each of these phase has a different interaction with the seismic structure of the crust and mantle and such structural effects will impose their own patterns on the radiation characteristics from the source. The range dependent component in the Lg/Pn and Sn/Pn ratios have been investigated for a dense set of three-component records covering the distance range out to 700 km, for an explosive shot in water in southern Sweden which formed part of the 1979 Fennolora experiment. A stable measure of amplitudes and amplitude ratios is provided by using the vector resultant of ground motion (the square root of the total energy). However, even for a common source there are significant variations in the amplitude ratios for Lg/Pn and Sn/Pn of a factor of three or more as a function of range. (cont.)

14. SUBJECT TERMS		15. NUMBER OF PAGES
Wave Propagation, Regional Phases, Pn, Sn, Refraction Studies, Heterogeneity, Discriminants		56
		16. PRICE CODE

17. SECURITY CLASSIFICATION OF REPORT	18. SECURITY CLASSIFICATION OF THIS PAGE	19. SECURITY CLASSIFICATION OF ABSTRACT	20. LIMITATION OF ABSTRACT
Unclassified	Unclassified	Unclassified	SAR

CONTINUATION OF 13. (ABSTRACT)

Three component record sections allow a detailed examination of the way in which individual records relate to the whole wavefields. The role of multiple reflections in building the Pg and Lg phases can be clearly seen as well as the complex substructure of the Pn and Sn phases returned from the uppermost mantle. This structure of the regional phases needs to be taken into account for accurate location of regional events. The vector nature of the wavefield is examined by using polarisation analysis and approximate decomposition of the wavefield into P, SV and SH contributions by removing the interactions with the free surface. Record sections of particle motion in the vertical and horizontal planes provide a useful complement to record sections for individual components of the field. The relative size of the SV and SH components estimated from the wavefield decomposition provides a better measure of the character of the source than a straight comparison of the cartesian components of motion.

INTRODUCTION:

This report describes a detailed study of a high quality regional dataset from the Fennolora Profile in Sweden. Fifty one three-component records for a single explosion in shallow water at the south of Sweden cover the distance range from 30-675 km. With such a dense recording system the evolution of the main regional phases Pg, Pn, Sg, Sn, Rg and Lg can also be used for polarisation analysis and other classes of three component processing.

The first part of the report:
> "On the nature of regional seismic phases - II 3-component studies of crustal and mantle phases"

has been submitted to *Geophysical Journal International*. This section is concerned with reconciling the nomenclature and methods of analysis used in refraction seismology with those commonly employed in discrimination work.

In seismic refraction the correlation of traces across a record section is very important and the analysis is concentrated on the detailed character of individual phases since the emphasis is on recovering seismic structure. Thus, for example, the Pn phase comprising P waves which have propagated through the upper mantle is recognised as having distinct substructure associated with the complexity of structure in the uppermost mantle. The interaction of the subphases give a significant variation in amplitude with distance with pronounced amplitude maxima and minima.

Most seismic trace analysis for discrimination work is based on the records from a single station or small array and so phase definitions are less precise than in refraction work. The Lg phase is normally associated with the largest amplitude on the record, but this point can be displaced by several second from the simple model commonly assumed for the travel time. Comparison of the record section results with the properties of individual records enable us to recognise the limitations of current phase association techniques.

With the detailed three-component sampling of the regional wavefield it is possible to undertake detailed polarization analysis including the construction of polarization record sections. The polarization properties of the main phases are quite stable with range and e.g. the onset of Sn can be detected most readily by an increase in motion in the horizontal plane. The three-component records also used to produce estimates of the P, SV and SH contributions to the wavefield via an approximate removal of the effect of the free surface.

Since the properties of comparable P and S phases are influenced by differences in the depth dependence of the P to S velocity ratio a survey of such ratio values has been compiled using data from Russian sources and from the limited number of long range refraction profiles for which both P and S velocity models are available.

The second part of the report:
> "The distance dependence of regional phase discriminants"

has been submitted for publication in the *Bulletin of the Seismological Society of America*. This study is based on the same three-component data as in part one but

concentrates on the distance dependence of the amplitude ratios Sn/Pn, Lg/Sn which could be used as measures of the character of a source. In this case all the records are for a single source type (an explosion in water) so that the range dependence can be extracted directly. The most stable measures of phase amplitude for each phase was found to be the resultant vector amplitude (related to the energy in the phase). The patterns for the Sn/Pn, Lg/Sn ratios are quite complex with variations of a factor of three or more. These arise in part from the amplitude maxima and minima due to the substructure of the Pn and tend to be amplified by the differing range dependence of the two S phases. Such variations in amplitude ratio are likely to be typical of regional paths and so comparison of source character is likely to be most reliable when carried out for sources at comparable distances with similar paths or else where observations are available at number of different ranges and azimuths.

On the nature of regional seismic phases - II . 3-component studies of crustal and mantle phases

B.L.N. Kennett
Research School of Earth Sciences, Australian National University,
G.P.O. Box 4, Canberra A.C.T. 2601, Australia

SUMMARY

The evolution of the main regional seismic phases with distance from the source is followed by exploiting three-component digital records from the Fennolora long range refraction profile in Sweden. Three component record sections, from an explosive source in shallow water, allow a detailed examination of the way in which individual records relate to the whole wavefields. The role of multiple reflections in building the Pg and Lg phases can be clearly seen as well as the complex substructure of the Pn and Sn phases returned from the uppermost mantle. The structure of the regional phases needs to be taken into account for accurate location of regional events.

The vector nature of the wavefield is examined by using polarisation analysis and approximate decomposition of the wavefield into P, SV and SH contributions by removing the interactions with the free surface. Record sections of particle motion in the vertical and horizontal planes provide a useful complement to record sections for individual components of the field. The relative size of the SV and SH components estimated from the wavefield decomposition provides a better measure of the character of the source than a straight comparison of the cartesian components of motion.

The interrelation of the P and S wavefields depends on the velocity ratio of the P and S waves, which varies significantly with tectonic setting. However, the character of the regional seismic wavefield is similar for classes of source as is illustrated by recordings of an earthquake and a quarry blast along a common linear array of seismometers in southeastern Australia.

Short title: 3-component studies of regional seismic phases

1. INTRODUCTION

A very large amount of effort has been expended on the analysis of seismic phases at regional distances in two distinct classes of study. Firstly, work on the determination of crust and upper mantle structure using seismic refraction profiles (see e.g. Luosto et al 1989 for a recent detailed study of a profile in northern Finland). Secondly, work on discrimination between natural and man-made sources for small events (see e.g. Pomeroy, Best & McEvilly 1982). Although both classes of work are directed at seismograms recorded at distances out to a few hundred kilometres from the source, the motivations have been very different and so attention has been directed at different aspects of the wavefield.

The object of this paper is to provide a link between the two different viewpoints by analyzing a set of three-component records from a long-range seismic refraction experiment (the Fennolora Profile in Sweden) with emphasis on the aspects of the regional wavefield which are of interest in the context of source discrimination. This requires an identification of the physical character of the wave propagation processes contributing to different parts of the seismogram, which is facilitated by having a dense sampling of the seismic wavefield. The use of three component records from a single source also allows an investigation of the stability of different aspects of the wavefield, such as e.g. polarization, as a function of range from the source.

2. THE REGIONAL SEISMIC WAVEFIELD:

The character of the seismic wavefield for distances from the source of a few hundred kilometers is dominated by the influence of the velocity structures within the crust and uppermost mantle. Another important contribution arises from the interaction of the different types of seismic waves with the free-surface. Regional S waves are generally totally reflected at the surface, whilst the corresponding P waves are converted to S waves with fairly high phase velocity which interact with structure deep in the upper mantle and so do not influence the wavefield out to 1000 km. The different patterns of surface reflection help to shape the evolution of the P and S wave components with distance.

Studies of seismic structure are based on an analysis of the details of seismic arrivals with emphasis on the correlations between successive seismograms in a record section display. The use of multiple seismograms, with a close spacing in distance, is very helpful in enabling specific types of arrival to be tracked across the record section, so that the influence of noise on individual seismograms can be reduced. The notation used to mark arrivals in such structural studies is designed to provide a detailed correlation between the classes of arrivals and the structural features which give rise to them.

In work directed towards source characterization, the available data may well consist of a set of seismograms from widely separated arrays or three-component stations. The local correlation properties of the wavefield across a small array can be exploited to extract estimates of the azimuth and horizontal slowness of the portions of the seismogram as a function of time. However, it is generally rather difficult to correlate arrivals between distinct recording sites because they lie at different ranges from the source. The major classes of arrivals on the seismogram are therefore recognized by their apparent slowness and time separation using a notation which does not attempt to take the interior structure of the phase groups into account. Kennett (1989 - Paper I) has

provided an operational description of the propagation processes which are associated with each of the major classes of crustal and upper mantle arrivals.

2.1 Seismic refraction data at regional distances:

A number of large scale seismic refraction experiments have been carried out with three-component recording to enable studies of both P and S wave structure to be carried for the crust and uppermost mantle. Thanks to the kind agency of Prof. K. Fuchs from the University of Karlsruhe we have been able to gain access to digital three-component data recorded along the Fennolora Profile in Sweden in the summer of 1979. Stangl (1990) has presented a compilation of all the data from the different shot points which provide detailed cover of crustal structure along a 1700 km profile the length of Sweden (Fig 1). We have used three-component data from shot point B to the south of Sweden and our analysis has concentrated on the zone out 800 km from the source. The shots at shotpoint B were fired in water and each shot was recorded on up to 152 recorders with a station spacing of approximately 10 km; the data quality is generally good because large charges were being used to secure propagation to beyond 1000 km.

In figure 2, we display a record section for each component of 51 three-component sets of traces for the shot B3N at Fennolora shotpoint B for distance ranges up to 675 km from the source. The traces have been filtered with a 4-pole Butterworth filter with 3 db points at 1 and 12 Hz. The trace amplitudes have been corrected for the scaling factors applied during digitization of the original analogue records and so true amplitude relations are available between components. A linear scaling with range has been applied to each record section to emphasize the arrivals at greater distance.

Stangl (1990) has made a detailed study of all the crustal and upper mantle phase data for the Fennolora experiment and has used reflectivity modelling to deduce one-dimensional models for the P and S velocity distribution with depth for the different shot points. We have used his model for shotpoint B (fig 4) to generate the record section of theoretical seismograms which is displayed in figure 3. The seismograms were generated using the WKBJ method, using generalized rays representing turning rays in the crust and upper mantle and reflections from the interfaces. Up to three surface reflections were included for each class of generalised rays. Superimposed on the theoretical seismograms for the vertical component of motion are the theoretical travel time curves for all the generalized rays which were included in the calculation, and also the phase designators commonly used in discrimination work. The frequency content of the synthetics is slightly lower than the observations, but it should be stressed that the object is to provide a guide to the interpretation of the observed seismograms rather than a detailed match. Nevertheless, Stangl's velocity model does a good job of representing the major features of the field.

Stangl's compilation of the detailed velocity models along the length of the Fennolora profile indicates significant lateral heterogeneity within the crust and upper mantle particularly on the northern part of the profile. The region of southern Sweden traversed by the waves recorded on the record section displayed in figure 2 shows little horizontal variation in properties, and so can be well represented using a one-dimensional model.

The major groups of arrivals which can be distinguished in figures 2 and 3 are the crustal phases Pg, Sg, Lg in which the dominant energy travels within the crust, and the

mantle phases Pn and Sn where much of the propagation path lies in the uppermost mantle.

2.1.1 Crustal phases

Pg: The Pg phase is characterized by a group velocity close to 6.0 km s^{-1}, and is built up from a number of different classes of processes. At distances out to the crossover for mantle phases (~190 km in figure 2) the Pg phase is composed of diving waves in the crust which are then reinforced at greater distances by reflections from the Moho. Crustal P wave multiples and multiple Moho reflections help to sustain the extension of the phase but as we can see from figure 2 it is difficult to discern beyond 450 km. The crustal velocities near the surface are quite high along the Fennolora profile (6.1 km s^{-1} at depths of a few hundred metres) and, in consequence, at a surface reflection only part of the P wave energy is directly reflected, and there is also efficient conversion of P wave energy to S waves which would have a turning point below 400 km depth. Such converted S waves are lost from the crustal waveguide. Where surface velocities are lower as e.g. in parts of the western United States the Pg phase can be observed to rather larger distances, because a greater proportion of the P wave field is reflected back from the surface as P.

The largest amplitude arrivals, which are likely to be associated with Pg by using array slowness measurements, are near the critical point for the Moho reflection (120-130 km in figure 2). This critical point energy is displaced from the theoretical travel time curve for Pg which is marked by the envelope of the travel time branches for different classes of P wave multiples. Differential times which depend on such an arrival could well be misleading.

Pg is generally most clear on the vertical component of motion but is also distinct on the radial component. Most transfer of P wave energy to the tangential component occurs due to heterogeneity along the propagation path and so the amplitude is small except near the Moho critical point.

Sg, Lg: The Sg phase at close range is entirely analogous to Pg and consists of refracted waves within the crust with reinforcement from the S wave reflection from the Moho. However, multiple S phases are very significant since the free surface acts as a perfect reflector for S waves with phase velocities lower than the surface P wave velocity. Such surface multiples tend to coalesce to produce a coherent arrival extending to large distances with a group velocity close to 3.5 km s^{-1} referred to as Lg. Figure 3 indicates the way in which the travel time curves for the multiple crustal S waves asymptote to define a single group velocity trajectory (3.56 km s^{-1}). Detailed reflectivity modelling for a horizontally stratified medium by Campillo, Bouchon & Massinon (1984) has confirmed the role of the multiples in shaping the character of the Lg arrival.

On an individual seismogram the Lg phase has a complex structure with, usually, no definite onset but a well defined amplitude maximum. The locus of the amplitude maxima lies slightly behind the envelope of the multiple S wave travel time curves. From figures 2 and 3 we can see the way in which the apparently continuous Lg wave phases is in fact built up from multiple Moho reflection branches so that the amplitude maximum can be displaced by a few seconds from the position given by the simple group

velocity relation. Such time displacements can be quite significant when the Lg arrival is used to define the location of an event.

Because the Lg phase is built up by interference between a range of different propagation processes it is rather sensitive to changes in structure along the path of propagation (see e.g. Bostock & Kennett 1990). However in regions of stable structure the Lg arrival can be recognized to beyond 1500 km from the source.

The Sg and Lg phases are generally clearly seen on all three components of motion and even for explosion sources can often be largest on the transverse component.

Rg: This arrival represents a Rayleigh wave propagating on the uppermost part of the crustal structure and cannot be simulated by the ray-based WKBJ calculations in figure 3. In figure 2 it appears as a lower frequency arrival which can be traced to about 100 km from the source. As the source was an explosion in water, the Rayleigh wave will not be generated directly and so Rg extends to shorter distances than for a land shot. In a horizontally stratified medium Rg would be confined to the vertical and radial components and usually has only a weak expression on the tangential component.

2.1.2 Mantle arrivals

Pn: The Pn phase group can be readily tracked across the record section in fig 2 as the first arriving energy beyond 200 km with a reduced time close to 6 s. This group of arrivals is transmitted through the crust at both source and receiver ends of the path, but the character of the phase is dominated by the influence of the structure in the uppermost mantle. Although the Pn phase group appears to have a nearly constant phase velocity of about 8.00 km s^{-1}, the structure of the arrivals is quite complex with significant amplitude variations with distance which can be associated with the interaction of the P waves with complex structure in the upper mantle (fig 4). Multiples of the Pn phase are generally of low amplitude because of the inefficiency of the P wave reflections at the free surface. The first multiple can just be discerned in the theoretical seismograms in fig 3, but is less clear in the observations (fig 2).

Pn is usually clear on both the radial and transverse components of motion but is normally very weak on the tangential component

Sn: The Sn phase is the S wave analogue of the Pn phase, whose properties are largely dictated by the S wave structure in the uppermost mantle. As noted by Gajewski et al (1990) the emergence of the Sn phase from the Sg arrivals is generally much less obvious than for the corresponding Pn arrivals. In Phanerozoic regions Sn, often has rather small amplitudes at the crossover with Sg and the amplitude builds up towards 300 km. However, in Precambrian regions exceptionally efficient S propagation can occur from explosive sources, and Sn can be easily recognized as it separates from Sg. Striking examples are provided in the S wave record sections published for the SVEKA refraction profile in southern Finland (Grad & Luosto 1987) and the Polar refraction profile in northern Finland (Luosto et al 1989) in which the Sn arrivals are of comparable clarity to Pn.

In figure 2, Sn is discernable, with a slightly lower amplitude than Pn even though Sg is strong. At the larger distances the SnSn multiple is also present (reduced time 83 s at range 600 km) because the efficient surface reflection for S means that the Sn energy is

returned to the upper mantle. The multiplicity of possible paths tends to increase the amplitude of SnSn relative to Sn (as can be seen in the theoretical seismograms in fig 3). As a result it is quite likely that at distances greater than 500 km from the source, SnSn may be picked instead of Sn (Kennett 1985).

Sn usually has its largest amplitude on the horizontal components of motion.

2.2 The vector character of the regional seismic wavefield

The set of three-component set of seismograms from the Fennolora experiment have sufficiently close spacing for the evolution of the different regional phases to be tracked, and so it is possible to look at the vector character of the wavefield in detail. We will consider two different approaches to the analysis of the character of the wavefield. The first is a decomposition of the vector wavefield into P, SV and SH components using the approximate technique for removing the free-surface interactions from the seismograms introduced by Kennett (1991). The second technique is the analysis of the polarisation character of the wavefield as a function of range by tracking the variation in particle motion in time at each recording position.

The seismic refraction profile was recorded with surface seismometers and so the surface wavefield includes the effects of amplification due to the interaction of the incident and reflected waves at the surface. For S waves there is also the possibility of phase distortion for waves incident at shallow angles than the critical angle for P waves. Kennett (1991) has shown that the inverse of the free surface interaction is a surprisingly simple operator, which for hard rock sites can be well approximated for slowness bands corresponding to the main regional phases. For the seismic refraction profile, the seismograms are already rotated to radial and transverse directions and this allows the transformation to be applied directly to the three-component records. Along the Fennolora profile there is a veneer of low velocity sediments of the order of 100 m thick, overlying material with P wave velocities around 6 km s^{-1}. Since the sediment cover is somewhat variable the approximate transformation of Kennett (1991) for surface velocities between 5.5 km s^{-1} and 6.3 km s^{-1} has been used directly. This transformation was designed for horizontal slowness bands, but such estimates are not available for the refraction profile and so we have worked with group velocity windows.

For Pn, (group velocities greater than 7 km s^{-1}) we have generated the estimates of the P, SV and SH amplitudes of the wavefield from the Z, R and T components as

$$P \approx -0.47\,Z + 0.25\,R, \qquad S \approx 0.43\,Z + 0.36\,R, \qquad H \approx 0.5\,T$$

where P is the P component, S the SV component, and H the SH component of the field. The transformation is frequency independent and therefore easily applied.
For the Pg part of the field (group velocities between 5.0 and 7.0 km s^{-1})

$$P \approx -0.50\,Z + 0.29\,R, \qquad S \approx 0.51\,Z + 0.28\,R, \qquad H = 0.5\,T$$

Over these two P wave intervals the exact expressions are slowly varying and so the approximations work well.

For the S wave windows the approximations are less satisfactory because the exact coefficients vary significantly with slowness, but they still allow some degree of balancing between the SV and SH contributions to the field For the Sn window (group velocities between 3.8 and 5.0 km s⁻¹), we use

$$P \approx -0.05\,H[Z] + 0.42\,R, \qquad S \approx 0.73\,Z - 0.06\,R, \qquad H = 0.5\,T$$

where $H[Z]$ indicates the Hilbert transform of the vertical component, this compensates for the phase distortion introduced by the surface. For the Lg waves (group velocities less than 3.8 km s⁻¹) the approximate transformation is

$$P \approx 0.19\,H[Z] + 0.49\,R, \qquad S \approx 0.85\,Z - 0.42\,R, \qquad H = 0.5\,T$$

The approximation for S is the least satisfactory of the set but does compensate to some extent for the relative suppression of the SV field (compared to SH) in the surface motion.

As an example of the success of this transformation to P, S, H components when applied to the three component records from the Fennolora profile we display in figure 5 the estimate of the P wave contribution to the wavefield. The time window covers the Pg and Pn phases as well as the short distance part of S; the transition between the different group velocity windows can just be seen as change in trace amplitude. The P waves are generally very well displayed which indicates that the calibration of the different components was very effective. The onset of Pg at short distances is muted because the approximation is not well tuned to direct arrivals. However the more distant portion of Pg where the reflection from the Moho is the principal contribution is well represented, and the surface multiple of the Moho reflection can now be clearly mapped at a reduced time around 15 s for ranges between 250 and 400 km. The transformation has enhanced the Pn waves and the character of the different wavegroups which make up the Pn group can now be clearly discerned. The amplitude of Pn shows significant variation with distance as the different wavegroups interact and we will look at this in more detail shortly.

It is more difficult to get a display with an equivalent representation of the mantle Sn phase because its amplitude is small compared with the strong Lg arrivals. Figure 6 shows the estimate of the SH contribution to the wavefield for a time window that covers Sg, Sn and part of Lg. Although the records are noisier than in figure 5 we can still see that Sn is not a simple arrival but has internal structure.

2.2.1 Polarization analysis

We can also make direct use of the three-component records of ground motion to look at other measures of the character of the vector wavefield. One such measure is the variation of particle motion with time and range from the source.

This particle motion can be displayed as a record section, as for example in figure 7 for the Pn phase which represents the motion in the vertical plane for the three-component records for the Fennolora shots B3N. In the upper panel in figure 7 we have plotted a 7 s time window of the P component of the Pn wavefield extracted from the three component records, and in the lower panel we show the particle motions on the same

scale as the seismograms so that the polarisation behaviour can be related directly to the wavefield. The particle motions over each 0.25 s interval in reduced time are plotted and are normalised by the peak amplitude along each trace. The vertical component of motion is plotted vertically, and motion in the radial direction is plotted horizontally as indicated by the small key diagram. The linear polarisation of the P wave onsets is distinct and tends to be followed by more complex behaviour as interference occurs between different wave groups.

A 7 s time window including the Pg phase is plotted in figure 8, with the P component in the upper panel and the particle motion plots for the vertical plane in the lower panel. The main Pg arrivals trend across the panel from 2 s reduced time at 100 km range to -2 s reduced time at 500 km range and can be followed by the linear polarisation of the particle plots. The surface multiple of the Moho reflection (at a reduced time of 2.5 s at 250 km) is enhanced in the P component plot compared with either the vertical (Z) or radial (R) components of motion, but can also be clearly recognised as a coherent arrival in the polarization record section.

As we have noted above, the Sn phase does not have as distinctive an onset as the Pn phase because it has to be picked against the coda of P. However Sn can be recognised by a change in the polarisation characteristics, since it is accompanied by a significant increase in motion in the horizontal plane. This is illustrated in figure 9. The upper panel of figure 9 displays the vertical component of motion for a 12 s time window around the Sn arrival which includes part of the Lg phase at smaller ranges. The lower panel shows the particle motion in the horizontal plane with motion in the radial direction plotted horizontally and motion in the tangential direction plotted vertically, as indicated by the small key diagram. The elliptical particle motion in Lg dominates the section out to 300 km. But, at greater distances, the Sn onset is mark by a sharp increase in the motion in the horizontal plane which correlates well with the arrivals on the vertical component. The horizontal amplitudes in the P coda are small and this enables a measure of amplitude in the horizontal plane to be used as an efficient detector for Sn.

The Lg phase is built up from multiply reflected S arrivals and these individual contributions to the phase show up well in the horizontal particle motion. In figure 10 we show an 11 s window around Lg in a similar configuration to figure 9, with vertical component seismograms above and horizontal particle motion below. There is a distinctive band of elliptical motion in both the vertical and horizontal planes associated with each of the multiple Moho reflections. For the Lg group the amplitude is generally sufficient to provide a clear detection but the nature of the arrival can be confirmed by exploiting the polarisation character of the arrival.

Each of the significant regional phases can be recognised by a consistent set of polarisation patterns with range from the source. The particle motion patterns tend to emphasise the way in which the Pg and Lg arrivals are built up from multiple reflections, and should not be regard as a single coherent phase.

2.2.2 Amplitudes of mantle phases

Gajewski et al (1990) have illustrated that Sn is commonly difficult to recognise for ranges just beyond the cross-over with Sg, whereas Pn tends to emerge from Pg which significant amplitude. We have seen above that a polarisation measure tends to enhance the detectability of Sn and it is therefore interesting to see how different

amplitude measures derived from the 3-component records compare for the P and S mantle phases.

We have compared the amplitude behaviour for each of the three cartesian components of motion with the amplitudes of the *P,S* and *H* components derived from the approximate wavefield decomposition procedure. We consider a 2 s window around the main arrivals associated with Pn and Sn and in figures 11 and 12 plot the maximum amplitude encountered for each component in that interval.

For the Pn arrival we note the general decline in amplitude with distance which is interrupted by significant local increases in amplitude which are most likely associated with changes in surface conditions. However, there are also broader scale amplitude fluctuations for each component which are likely to arise from deeper structure. The vertical and radial components usually have comparable amplitudes but after removal of the free surface effects the *P* component dominates, as would be expected, after the emergence of Pn from Pg at 200 km range. Variations in the surface conditions lead to local variations but beyond 250 km the amplitudes of the *S* and *H* components are similar.

For Sn the amplitudes are usually larger on the transverse component than the radial despite the fact that the source was an explosion in water. This arises, in part at least, from the larger amplification of SH waves at the free surface. After the approximate corrections for the influence of the free surface have been applied the disparity in the apparent size of the motion in the vertical and horizontal planes are removed and now the amplitudes of the *S* and *H* components are similar. The application of the wavefield transformation has provided a better measure of the nature of the original source radiation than the observed particle motion.

Within the Pn and Sn wave groups we have noted a significant variation in the patterns of the amplitude distribution in time and distance (figs 5,6,12,13). Such variability has been recognised on other profiles and has been interpreted in terms of complex structure within the uppermost mantle (Kind 1974, Fuchs & Schulz 1976) manifested by a sequence of overlapping arrivals. For the Fennolora data, Stangl (1990) has inferred the substructure of the Pn and Sn phases by detailed correlation between traces using the full dataset, and has then matched the observed behavior using the reflectivity method to produce a velocity model for the mantle. The P and S wave velocity profile for shotpoint B is plotted in fig 4 along with the P/S velocity ratio. The general character of the P and S wave distributions are similar but there is a noticeable difference between the P/S velocity ratio in the mantle above 80 km depth and that beneath. At larger distances (beyond 700 km) where the contribution to the onset of Sn comes from below 80 km there will be a change in the distance dependence of the Pn/Sn amplitude ratio. The actual situation is compounded by the existence of lateral variations in P wave velocity in the crust and uppermost mantle and topography at the core mantle boundary.

2.3 P/S Velocity ratios

In the previous section we have been able to provide a detailed analysis of the regional wavefield in one region. The extension of such results to other situations depends on the stability of the relation between the characteristics of the P and S wavefields.

For the crustal phases, the relative velocities of the Pg and Lg phases will be controlled by the ratio of P wave to S wave velocities (α/β). Changes in velocity gradients will also influence the detailed amplitude distributions but the strongest influence on the character of these phase is the surface P wave velocity, as noted above Pg is sustained to large distances as the surface P wave velocity diminishes. For the mantle phases, the relative visibility of Pn and Sn will depend on the relation of the P and S velocity structure at the top of the mantle. For many regions the P wave structure is well established but the S velocities are less well controlled.

Within Eurasia, an extensive program of long-range explosion seismology on the territory of the former U.S.S.R has produced a good deal of information on crustal and upper mantle structure. P wave models have been published to depths of 200 km or more but also S wave models for the crust and uppermost mantle. However only a small fraction of the data has been presented in the form of record sections along a profile (especially for S). A notable exception is the paper by Tarkov & Basula (1983) which displays both P and S record sections out to 300 km from quarry blasts in the Voronezh shield to the south of Moscow. From this work and other Russian compilations (Alekseev et al 1988) we can build up a picture of the correlation of P and S wave velocities in the crust and upper mantle. Figure 12 illustrates the behaviour of the ratio of P wave to S wave velocities (α/β) as a function of P wave velocity (α) for a number of different regions of Eurasia. There are substantial differences in the S wave velocities for the same P wave velocity in both the crust and uppermost mantle even where the tectonic settings are comparable. The variability of the velocity ratio within the Voronezh shield on profiles with different orientation suggests influence of anisotropy on S wave velocities.

These velocity ratio results can be supplemented by results from long range refraction profiles in Europe. Assumpção & Bamford (1978) have carried out a detailed study along the LISPB profile in Scotland, Grad & Luosto (1987) and Perchuc (1992) have analysed the P/S velocity ration on the SVEKA profile in southern Finland, and Stangl (1990) has generated an extensive compilation for the full Fennlora profile in Sweden. The P/S velocity ratios from these long range refraction profiles are plotted in figure 13 in the same format as used for the Russian results in figure 12. The velocity ratios in the upper crust are similar for Scotland and the Fennoscandian profiles, but the ratios are lower for the middle and lower crust under Scotland.

2.4 Regional phases and event location

The detailed record sections presented above show that the detailed structure of the regional wavefield should not be neglected. Even though a arrival has been identified from the analysis of a regional array as belonging to one of the major classes of arrival (Pn, Pg, Sn, Lg) an effort should be made to make a correlation with a physical propagation process rather than resort to an empirical traveltime table. As we have seen the actual arrival detected by a station can be displaced by several seconds from the emprical Pg or Lg traveltime relations.

The array identifications, based on phase velocity filtering, are very effective for preliminary locations, but once the approximate distance from the source is known it is desirable to make a correlation with a physical ray path. This can be achieved by applying a group velocity filter to the traveltimes calculated for a regional velocity model,

including surface multiple phases. Such a procedure requires only a minor modification to the output of most travel time routines and enables array data to be used alongside readings from single stations.

For the phases Pn and Sn, the structure of the event is quite complex but the assumption of a simple travel time curve, without allowance for the detailed substructure of the phases will generally be adequate for the purposes of event location out to 500-600 km from the source. At larger distances it may well be necessary to make a more detailed allowance for the structure in the upper part of the mantle.

2.5 Dependence of the regional wavefield on source characteristics

The closely spaced record sections for the regional seismic wavefield depicted in figure 2 are for one type of source (an explosion in water), but allows a detailed investigation of the influences of structure on the character of the regional phases which should be common to different source types. Unfortunately such detailed observations are generally not available for natural sources.

During LISPB experiment in 1974 an earthquake in Western Scotland was recorded along the north-south refraction profile (Kaminski et al 1976), giving coverage for the distance range 70 to 290 km from the event, the general patterns of propagation were consistent between the P and S wavefields.

During the operation of a linear array of short-period digital seismometers in southeastern Australia during the southern summer of 1989/1990 we were fortunate enough to record both an earthquake (FF) and a quarry blast(SM) which lie along the line of the profile (see fig 14). The record sections for the vertical components of motion for the two events are displayed in figure 15. The general character of the wavefield is similar for the two different types of events, although there are differences in the P radiation (by fortunate accident a nodal plane for the P wave radiation from the Fitzroy Falls earthquake passes through the line of the array). On each section we can see the change in phase velocity with the emergence of the Pn arrivals, but the corresponding emergence of Sn cannot be tracked reliably. The amplitude of the P coda is quite high and there is little difference in frequency content between the P and S wave fields. The Lg phase is well represented for both events and is of slightly shorter duration for the man-made source.

This example reinforces the advantage of multistation recording in understanding the character of the regional wavefield, even where the station spacing is not very close. The arrivals correlate well across the main array and the phases can therefore be readily identified. Even for the isolated distant station the identification of the features on the seismogram is simplified by extrapolation from closer ranges.

In the period after the installation of a new regional station it is highly desirable to build up a record section from available source so that the structure in the neighbourhood of that station can be calibrated.

3. DISCUSSION

A number of the techniques which have been proposed for discriminating between different types of seismic sources at regional distances depend on the relative amplitudes of different P and S phases. Ideally the P and S phases which are being compared should have similar propagation characteristics, so that amplitude differences can be ascribed to

the variation in the radiation at the source. The crustally guided waves Pg and Sg can be used to some extent out to 200-300 km from the source but Pg is frequently difficult to track to larger distances. For the distance zone from 200-1000 km away from the source, the main arrivals are Pn, Sn and the superposition of crustally guided S waves denoted by Lg in discrimination work. Lg is frequently the largest phase on seismic records out to 1000 km but it is known to be sensitive to variations in crustal structure and so can be only used as an S reference when the propagation paths from different sources are very similar.

An additional complication in the comparison of Pn and Lg as proposed by Blandford (1980) comes from the very different sampling of the source by the two phases. Pn and Sn waves leave the source in relatively narrow angular range with horizontal slowness close to the reciprocal of the P or S wave velocities in the uppermost mantle. Whereas the Lg phase is built from the superposition of a wide range of S wave multiples and thereby includes a broad angular spectrum of S waves leaving the source to be trapped in the crust. This may help to reduce the influence of S nodal patterns on a single Lg amplitude measurement, but the Pn amplitude will still be susceptible to the accidents of source orientation.

The observational studies from long-range refraction studies with simple sources indicate that wave propagation through the uppermost mantle is much more complex than is assumed in the simple phase interpretation commonly adopted in the context of source discrimination. The Pn and Sn phases have a delicate sub-structure which reflects the velocity structure in the upper part of the mantle. Variations in the P/S velocity with depth will lead to changes in the amplitude ratio for Pn/Sn as a function of distance.

The approximate wavefield decomposition of Kennett (1991) provides a useful measure of the relative contribution of the SV and SH parts of the wavefield because the major part of the free surface amplification effects have been removed.

References

Alekseev A.S., Egorkin A.S. & Pavlenkova N.I., 1988, Shear waves in lithosphere studies on the territory of the U.S.S.R., *Tectonophys.*, **154**, 227-239.

Assumpção M & Bamford D. (1978) LISPB V. - Studies of crustal shear waves, *Geophys. J. R. astr. Soc.*, **54**, 61-73

Blandford R.R. (1980) Seismic discrimination problems at regional distances, in *Identification of Seismic Sources - Earthquake or Underground Explosion*, eds Husebye E.S & Mykkeltveit S., 695-740, Riedel, Dordrecht.

Bostock M.G. & Kennett B.L.N. 1990, The effect of 3-D structure on Lg propagation patterns, *Geophys. J. Int.*, **101**, 355-365.

Campillo M., Bouchon M. & Massinon B., 1984, Theoretical study of the excitation, spectral characteristics and geometrical attenuation of regional seismic phases, *Bull. seism. Soc. Am.*, **74**, 79-90.

Egorkin A.V., S.K. Zuganov, Pavlenkova N.A. & Chernyshev N.M. 1987 Results of lithospheric studies from long-range profiles in Siberia, *Tectonophys.*, **140**, 29-47.

Fuchs K. & Schulz K., 1976, Tunneling of low-frequency waves through the subcrustal lithosphere, *J. Geophys.*, **42**, 175-190.

Gajewski D., Stangl R., Fuchs K. & Sandmeier K.J., 1990, A new constraint on the composition of the topmost continental mantle - anomalously different depth increases of P and S velocity, *Geophys. J. Int.*, **103**, 497-507.

Grad M. & Luosto U., 1987, Seismic models of the crust of the Baltic shield along the SVEKA profile in Finland, *Annales Geophysicae*, **5 B**, 639-650

Kaminski W., Bamford D., Faber S., Jacob B., Nunn K., Prodehl C., 1976, A lithospheric profile in Britain II - A preliminary report on the recording of a local earthquake, *J. Geophys.*, **45**, 255-372.

Kennett B.L.N., 1989, On the nature of regional seismic phases - I. Phase representations for Pn, Pg, Sn, Lg, *Geophys. J. R. astr. Soc.*, **98**, 447-456.

Kennett B.L.N., 1991, The removal of free surface interactions from three-component seismograms, *Geophys J. Int.*, **104**, 153-163.

Kind R., 1974, Long range propagation of seismic energy in the lower lithosphere, *J. Geophys.*, **40**, 189-202.

Perchuc E. 1992, Distribution of Vp/Vs in the crystalline complex Earth's crust on SVEKA profile, *Phys. Earth. Planet. Int.*, **69**, 239-245.

Pomeroy P.W., Best W. J. & McEvilly T.J., 1982, Test ban treaty verification with regional data - a review, *Bull. seism. Soc. Am.*, **72**, S89-S129

Stangl R., 1990, Die Struktur der Lithosphäre in Schweden, abgeleitet aus einer gemeinsamen Interpretation der P- und S-Wellen Registrierungen auf dem FENNOLORA-Profil, *Doktors der Naturwissenschaften Thesis*, University of Karlsruhe.

Tarkov A.P. & Basula I.P., 1983, Inhomogeneous structure of the Voronezh shield lithosphere from explosion seismology data, *Phys. Earth. Planet. Int*, **31**, 281-292

Yegorkin, A.V. & Chernyshov N.M., 1983. Peculiarities of mantle waves from long range profiles, *J. Geophys.*, **54**, 30-34.

Figures:

Fig 1. The configuration of the 1979 Fennolora experiment in Sweden, the three-component digital data displayed in figure 4 is from shotpoint B to the south of Sweden.

Fig 2. Three component record sections for recorders across the southern part of Sweden, extracted from three-component data for the shots B3N at Fennolora shotpoint B. The seismograms are plotted with true amplitudes and a linear display gain in range.
a) vertical component, b) radial component, c) transverse component

Fig 3. Vertical component synthetic seismograms calculated using the WKBJ technique for the velocity model proposed for Fennolora shotpoint B by Stangl (1990) - see fig 4. The theoretical travel times and the phase designations used in discrimination work are superimposed to provide a key to the interpretation of the observed record section in fig 2.

Fig 4. The depth variation of P and S wave velocities, and their velocity ratio, for the long range profile from shotpoint B on the Fennolora profile in Sweden (Stangl 1990).

Fig 5. Record section of the P component of the wavefield estimated by the removal of free surface interactions from the three-component records. The time window is centred on the Pn phase.

Fig 6. Record section of the H component of the wavefield estimated by the removal of free surface interactions from the three-component records. The time window is centred on the Sn phase.

Fig 7. Polarization record section for a time window around the Pn phase. The upper panel displays the P component of the wavefield, and the lower panel displays particle motion plots for 0.25 s intervals along each trace.

Fig 8. Polarization record section for a time window around the Pg phase. The upper panel displays the P component of the wavefield, and the lower panel displays particle motion plots for 0.25 s intervals along each trace.

Fig 9. Polarization record section for a time window around the Sn phase. The upper panel displays the vertical component of the wavefield, and the lower panel displays particle motion plots for 0.5 s intervals along each trace.

Fig 10. Polarization record section for a time window around the Lg phase. The upper panel displays the vertical component of the wavefield, and the lower panel displays particle motion plots for 0.5 s intervals along each trace.

Fig 11. The dependence of the maximum amplitude of the Pn phase group as a function of range. The upper panel shows the cartesian components of motion and the lower the wavefield components extracted by the approximate removal of free surface effects.

Fig 12. The dependence of the maximum amplitude of the Pn phase group as a function of range. The upper panel shows the cartesian components of motion and the lower the wavefield components extracted by the approximate removal of free surface effects.

Fig. 13. Variation of the ratio (α/β) of P wave to S wave velocity as a function of P wave velocity (α) for different regions of Eurasia from Soviet studies: UR- the Urals, Kaz - the Kazakh fold belt, TS - the Tien Shan, SP - the Siberian Platform, WS - west Siberian plate, VD - Vilyui depression (Siberia), V1,V2,V3 - the Voronezh Shield (Russia).

Fig. 14. Variation of the ratio (α/β) of P wave to S wave velocity as a function of P wave velocity (α) for different regions of Europe from long range refraction profiles: Fl - the Fennolora profile (Sweden), FSv- the SVEKA profile (Finland), Br - the LISPB profile .

Fig. 15. Location map for the digital array in southeastern Australia which recorded the Fitzroy Falls earthquake (FF) and the South Marulan quarry blast (SM) shown in fig 16.

Fig 16. Vertical component record sections for the earthquake and quarry blast. In each case the Pn phase can be clearly observed, even though the line is close to nodal for the earthquake, it is much more difficult to detect the Sn arrival even with a number of records.
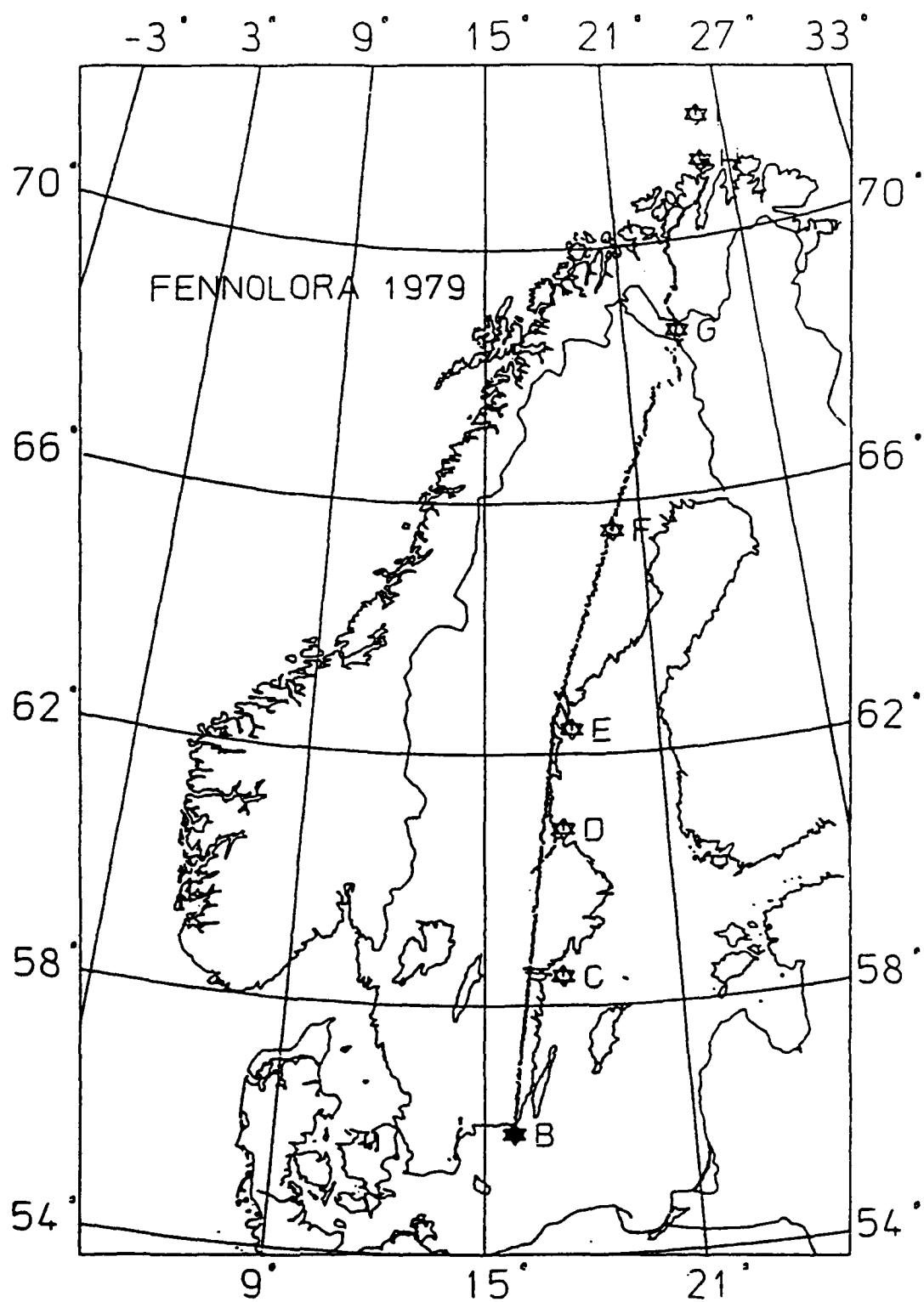
FIGURE 1

ZC - fennl obs

T - Range/8.0 [s]

Range [km]

19
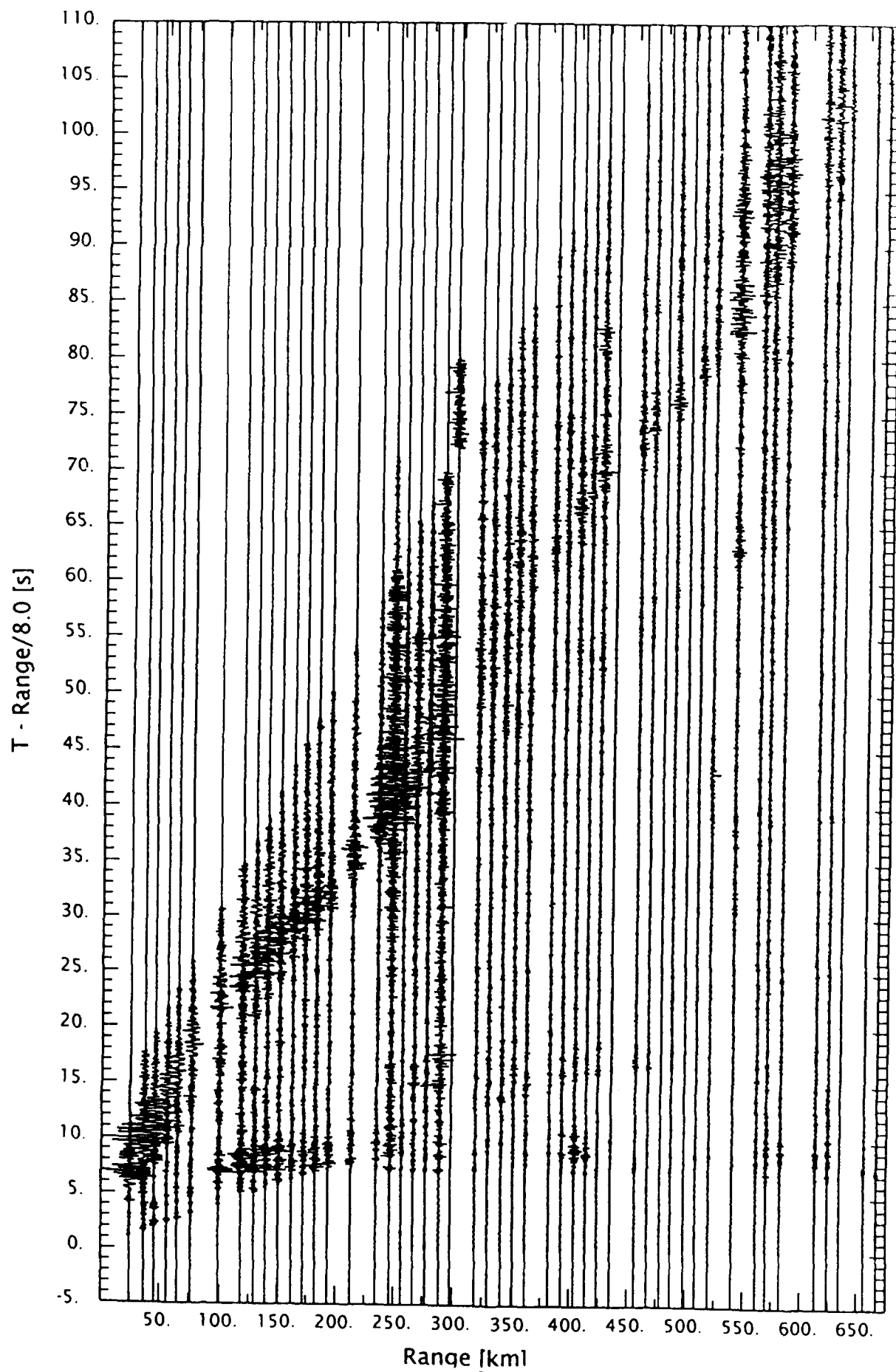
FIGURE 2

RC - fennl obs
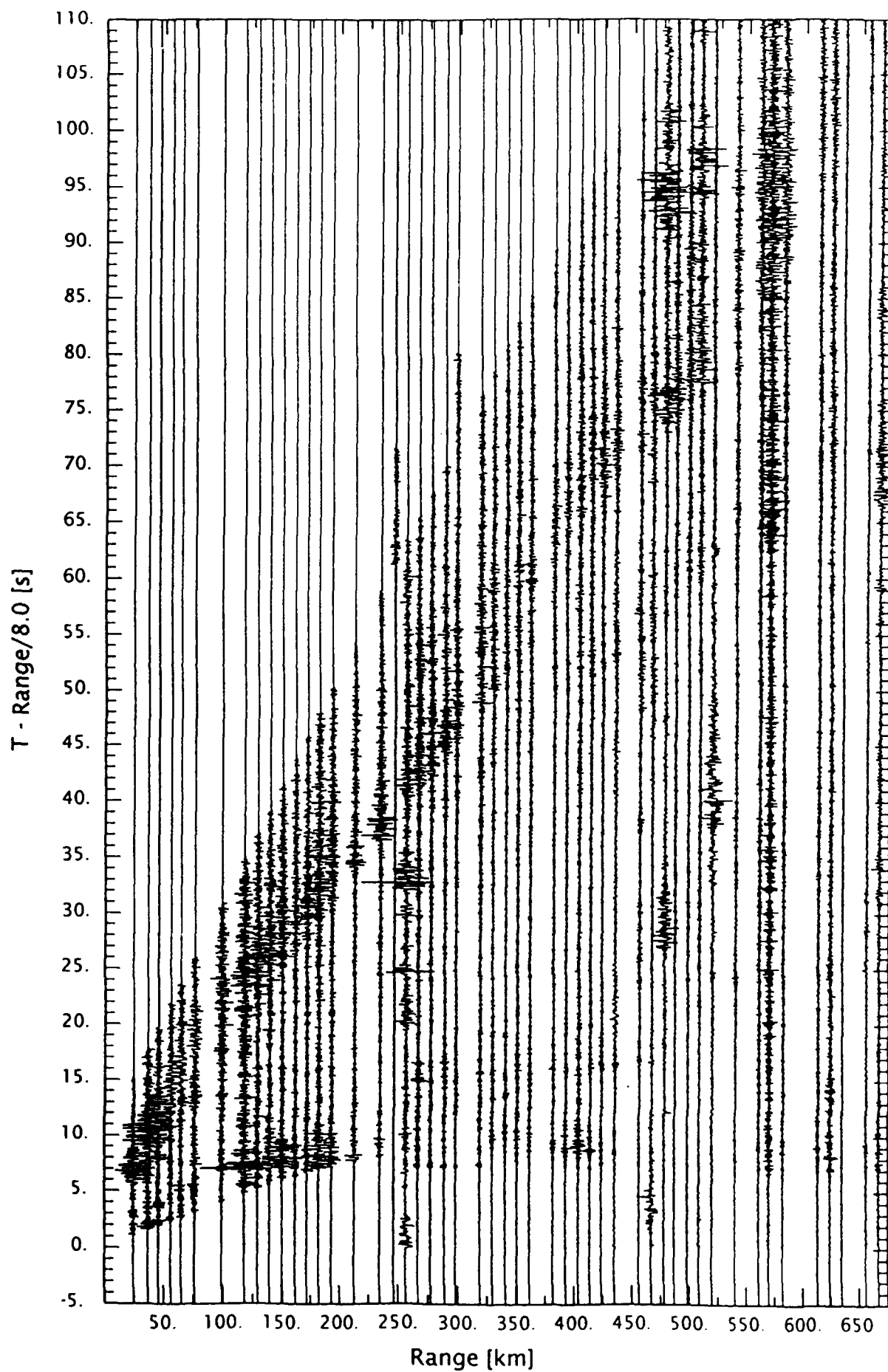
FIGURE 2
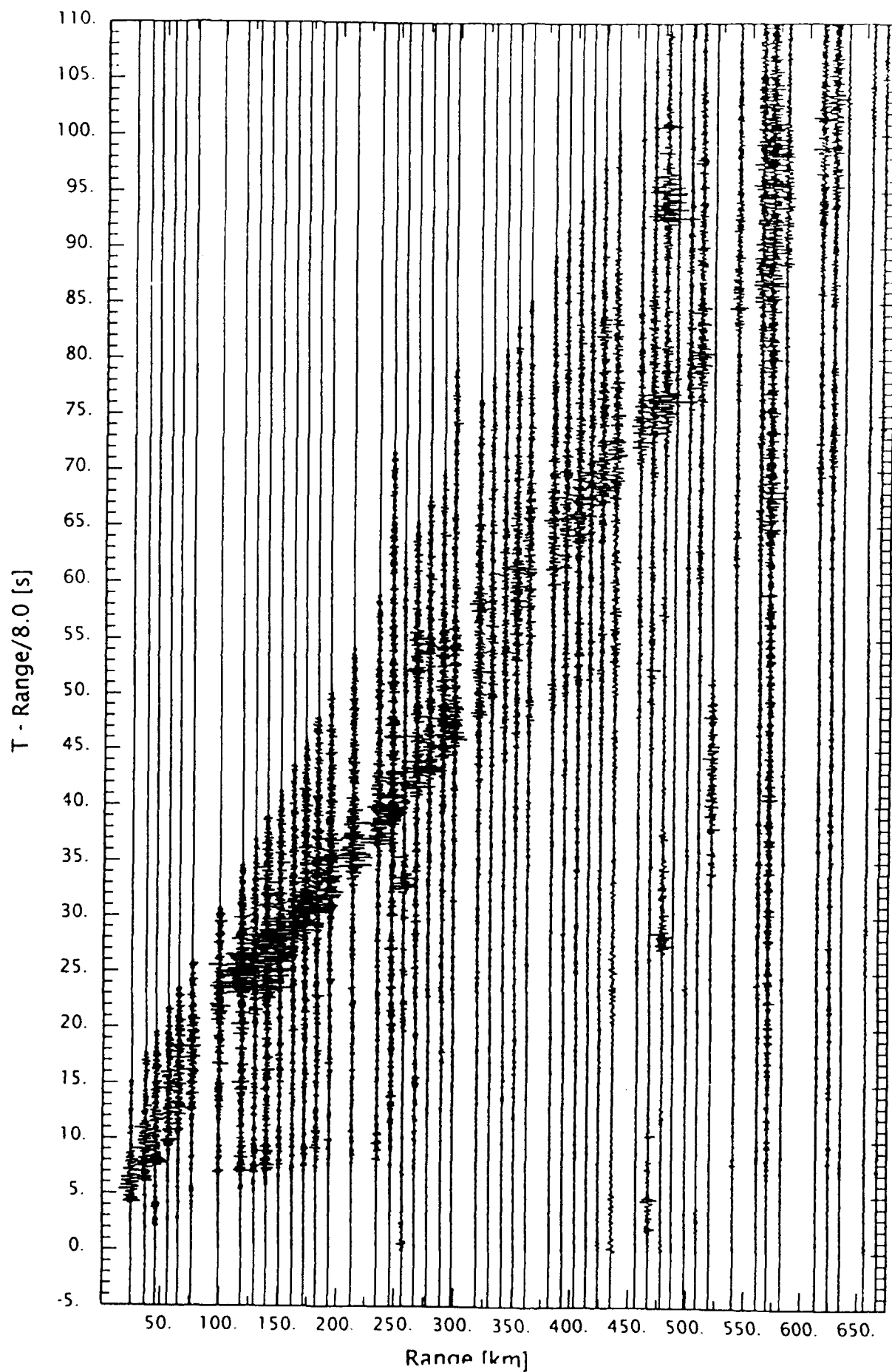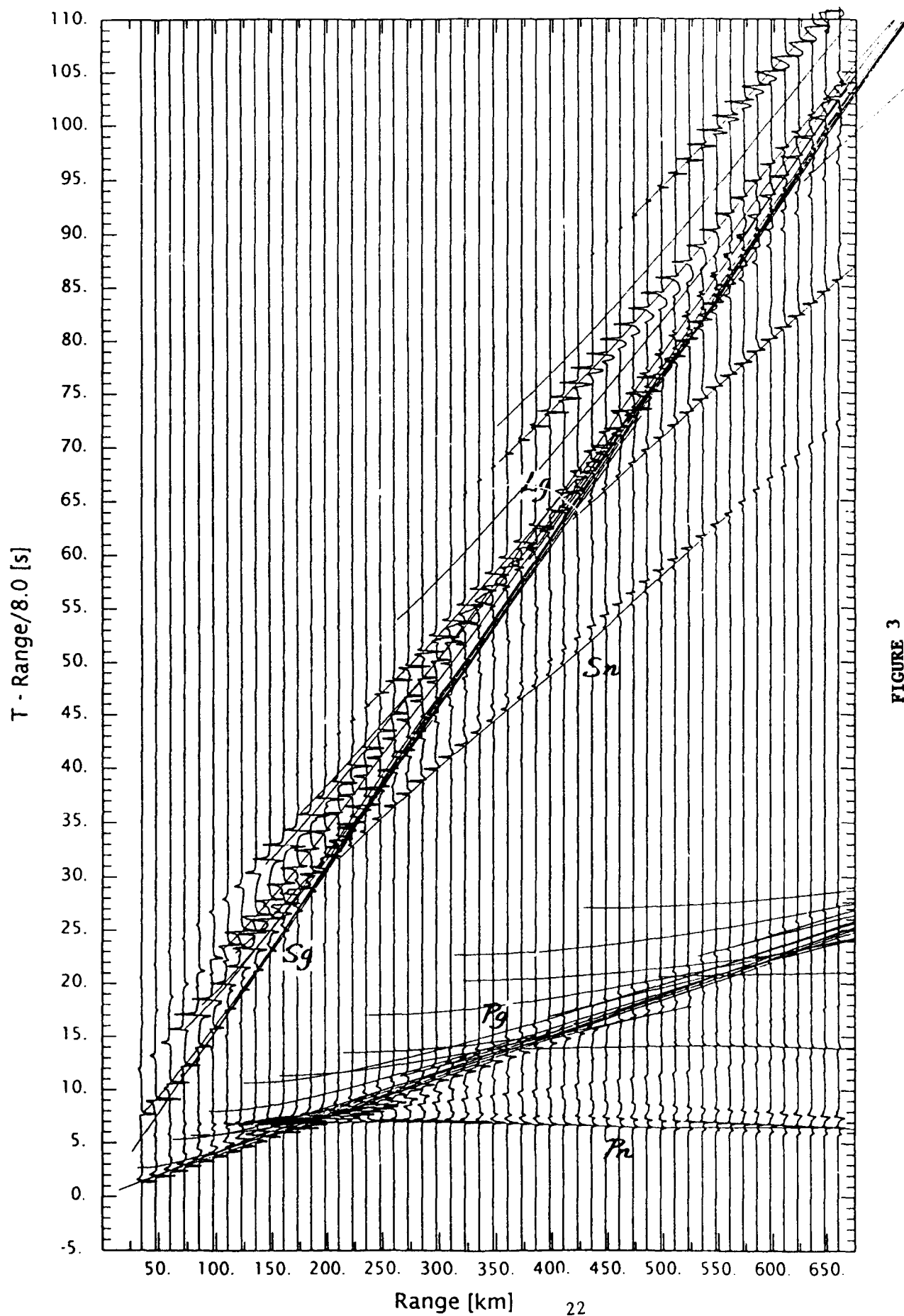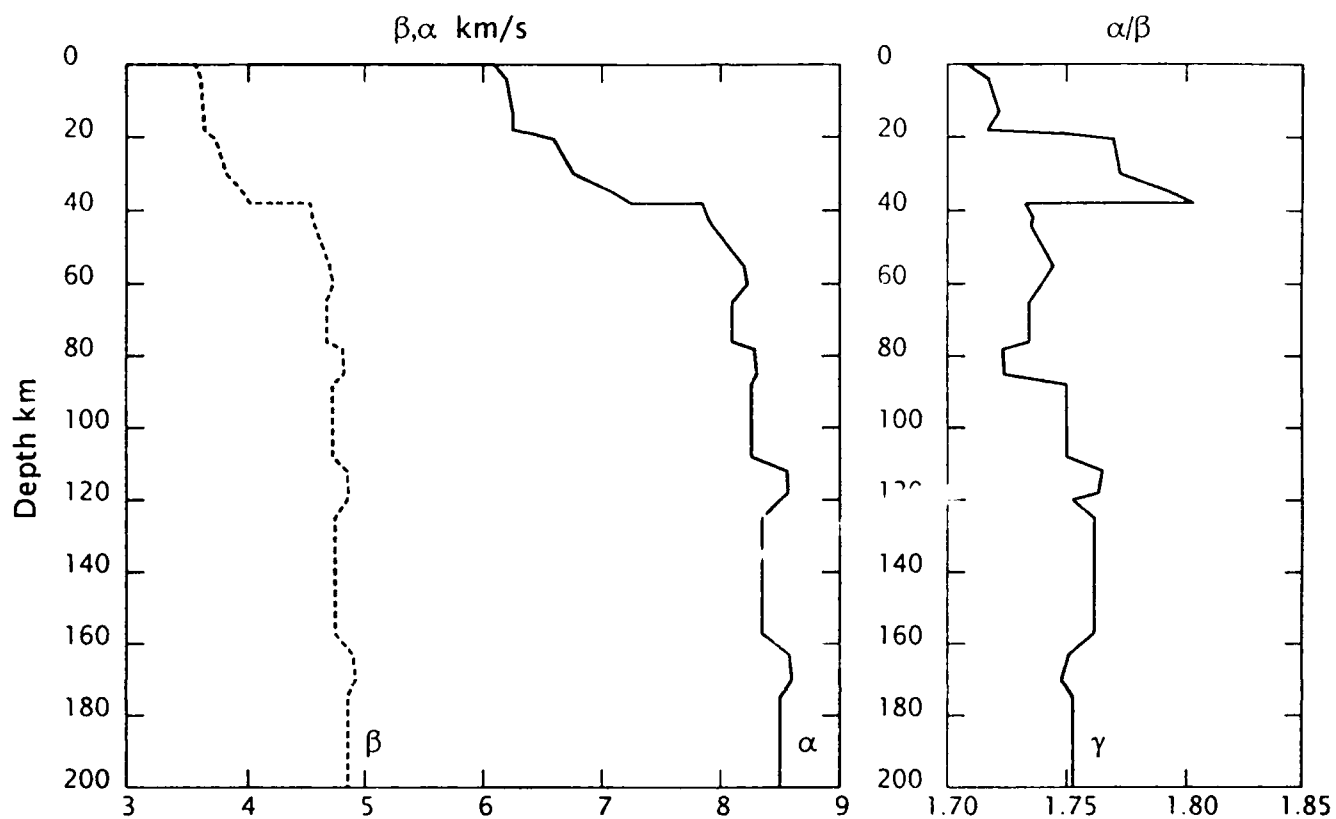
20

TC - fennl obs

T - Range/8.0 [s]

Range [km]

FIGURE 2

P&S - fennl

FIGURE 3

22

β,α km/s

α/β

Depth km

0
20
40
60
80
100
120
140
160
180
200

β

α

3   4   5   6   7   8   9

0
20
40
60
80
100
120
140
160
180
200

γ

1.70   1.75   1.80   1.85

FIGURE 4

4

P Component

Range [km]

FIGURE 5

T - Range/8.0 [s]

H Component

Range [km]

FIGURE 6

T - Range/4.5 [s]

TC

P component

FIGURE 7

P component

FIGURE 8

27

z C Seismograms

zc

Horizontal Plane

FIGURE 9

9

28
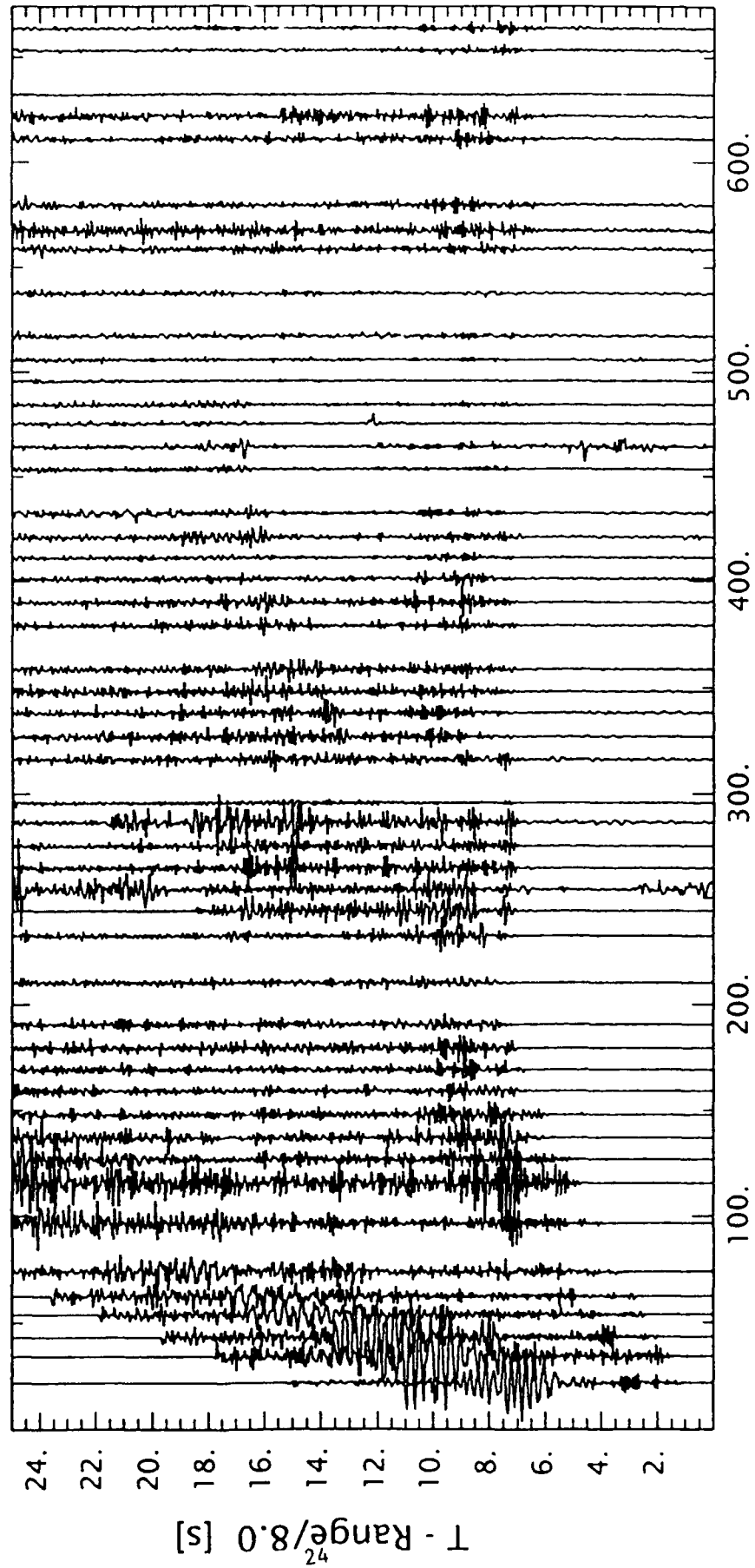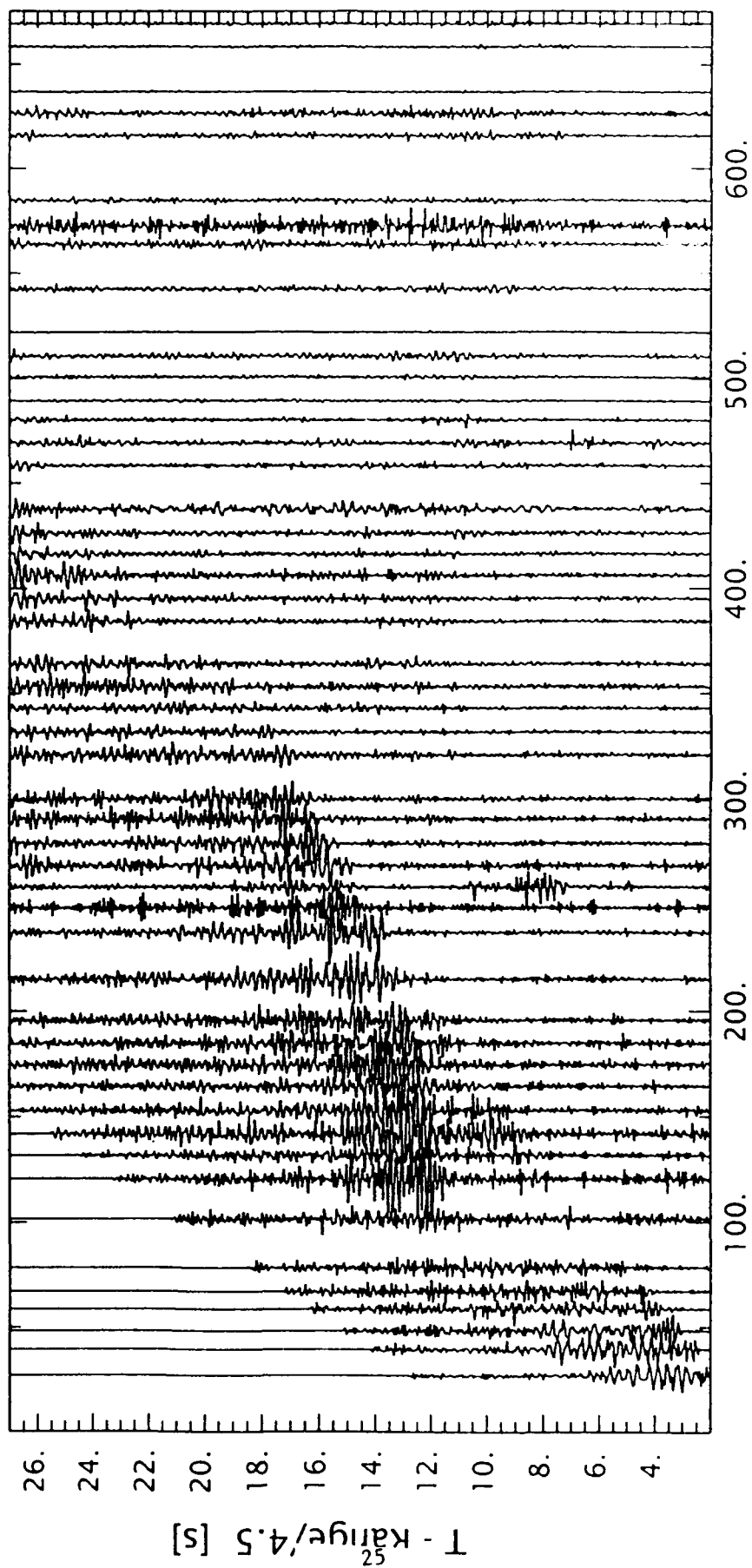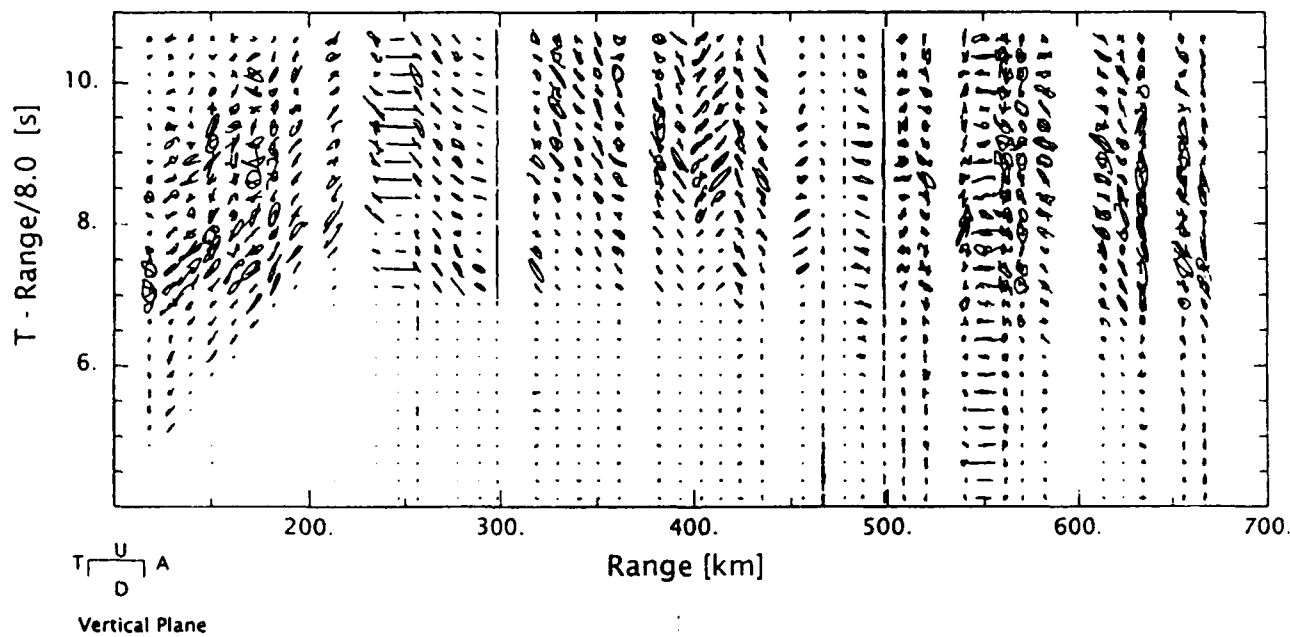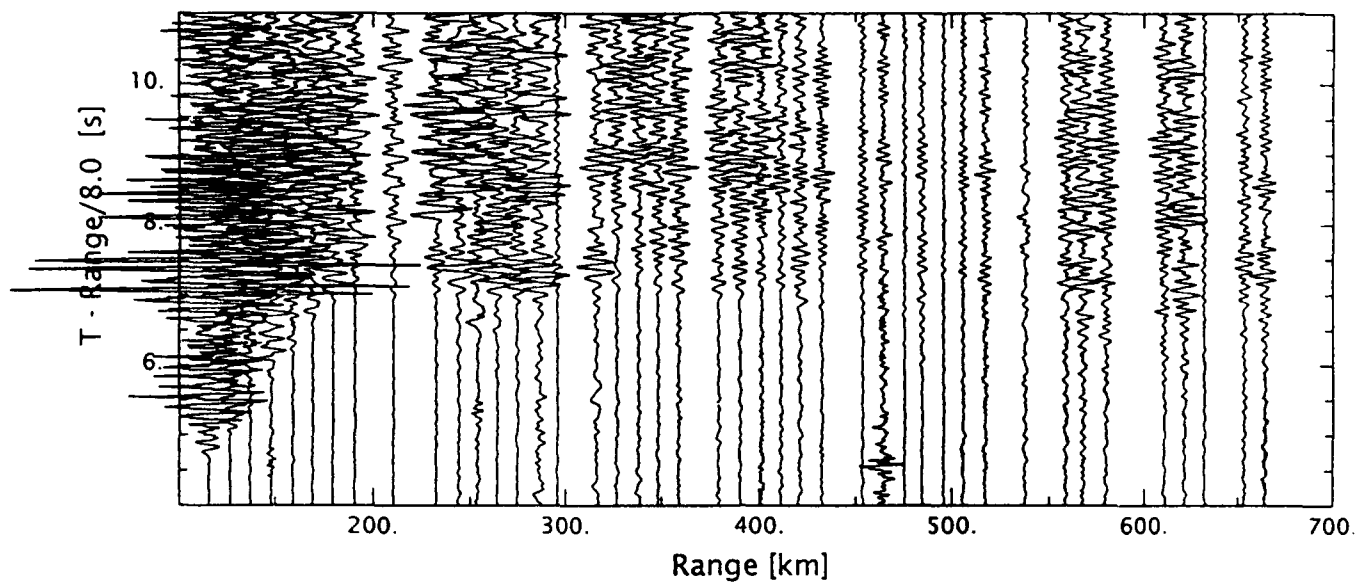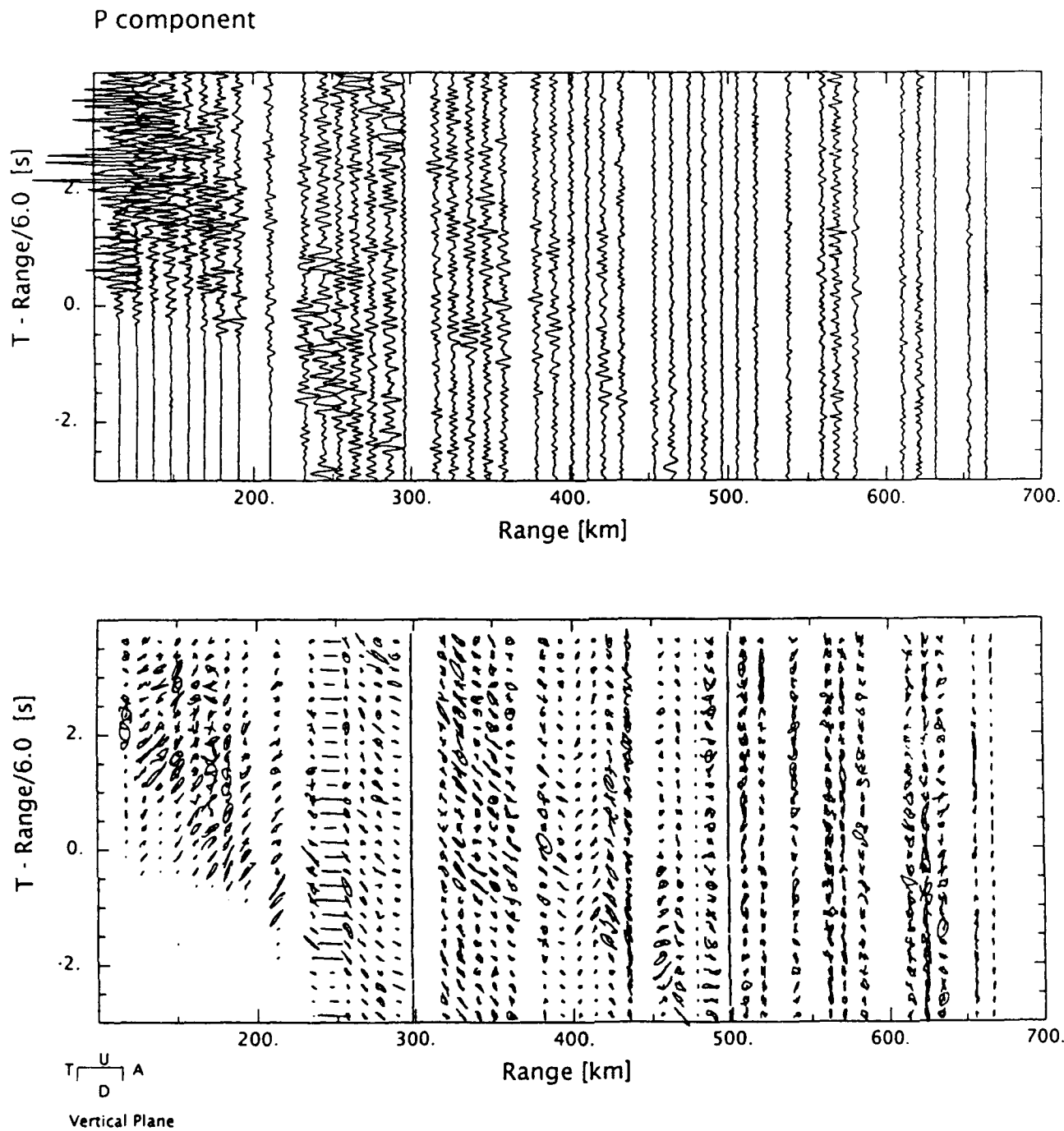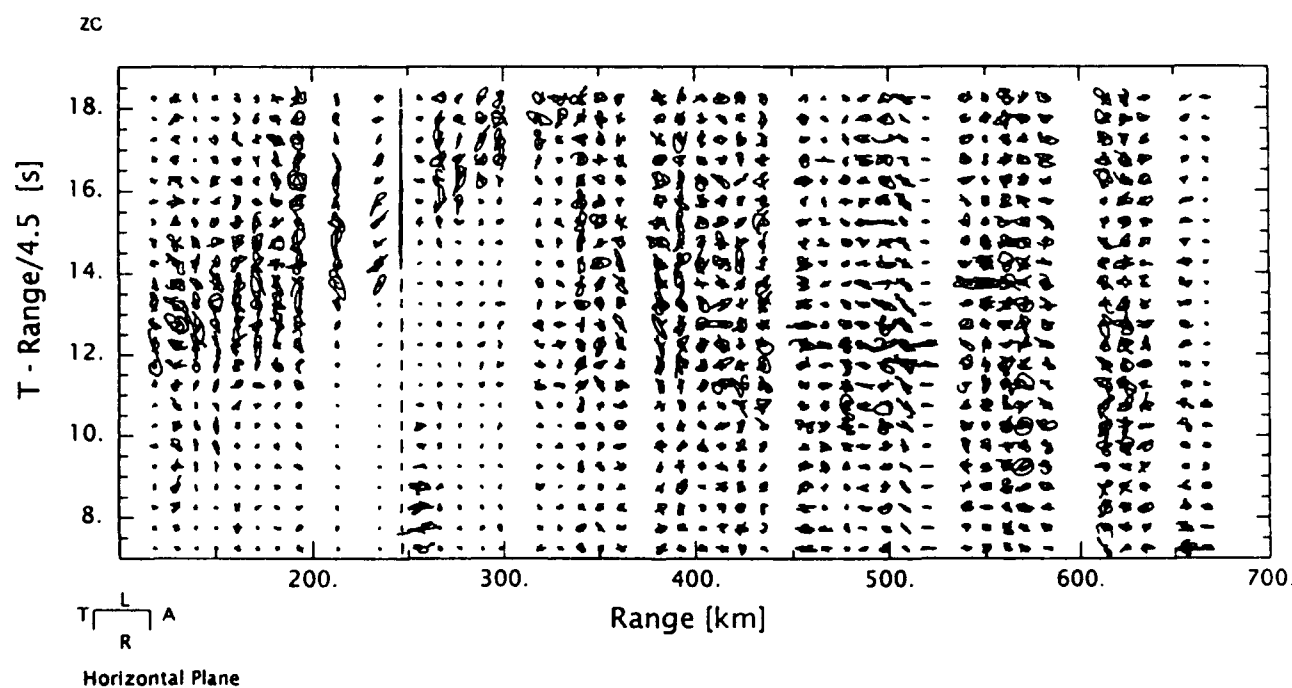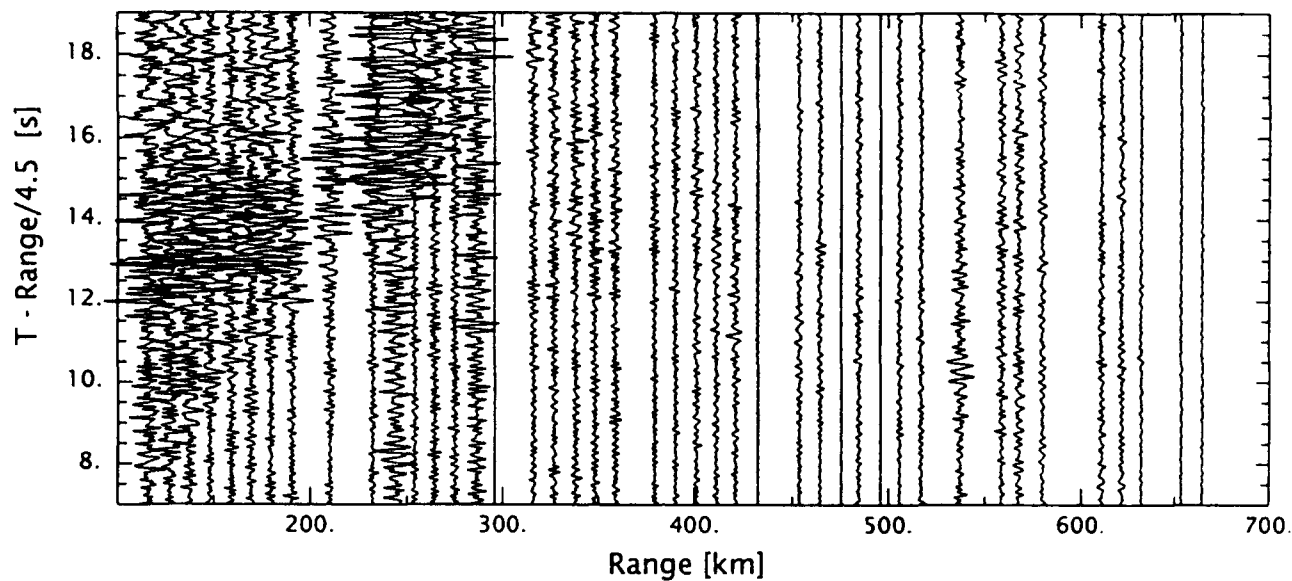
Z C Seismograms

FIGURE 10

10

Pn

Pn - wd
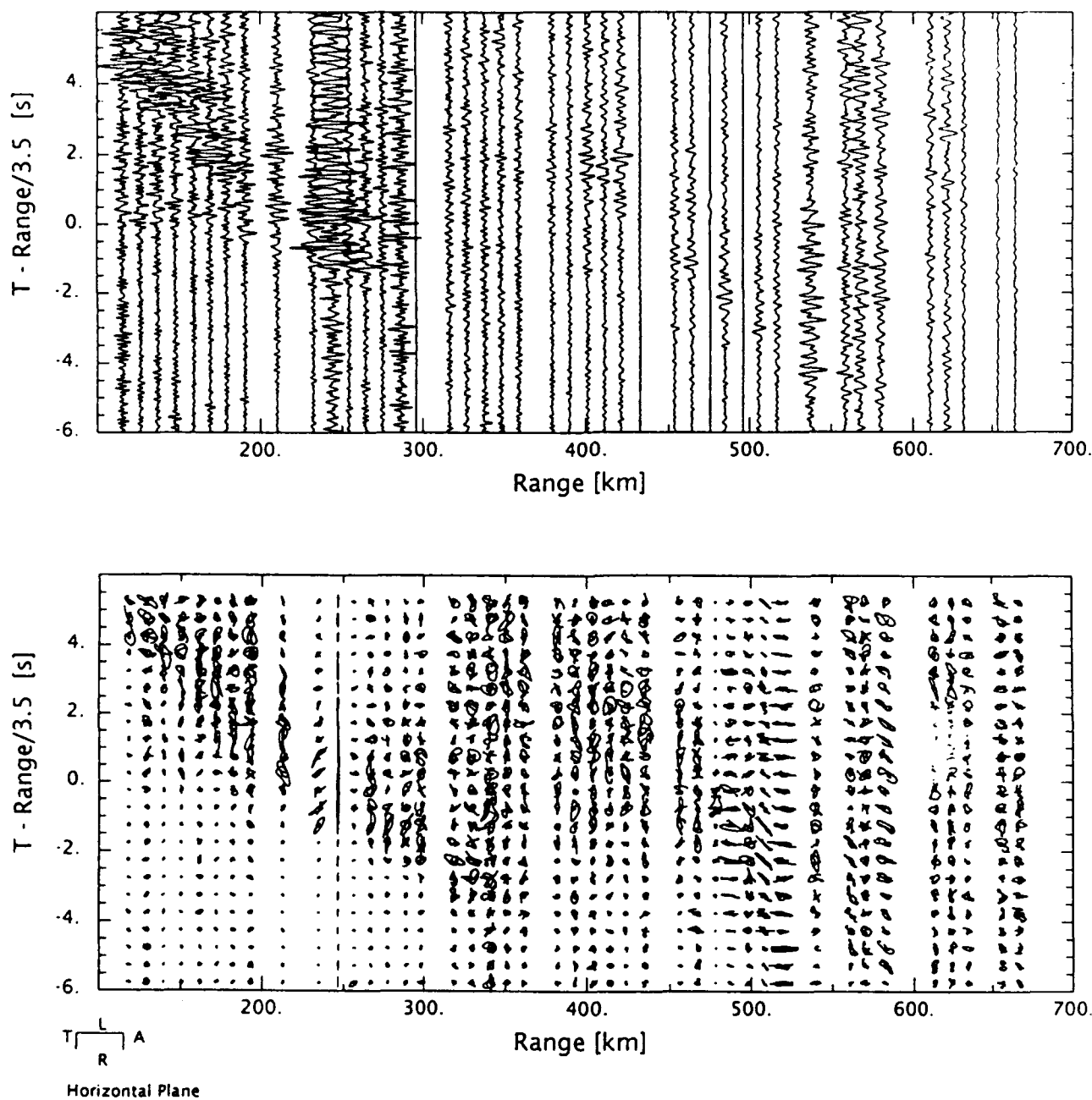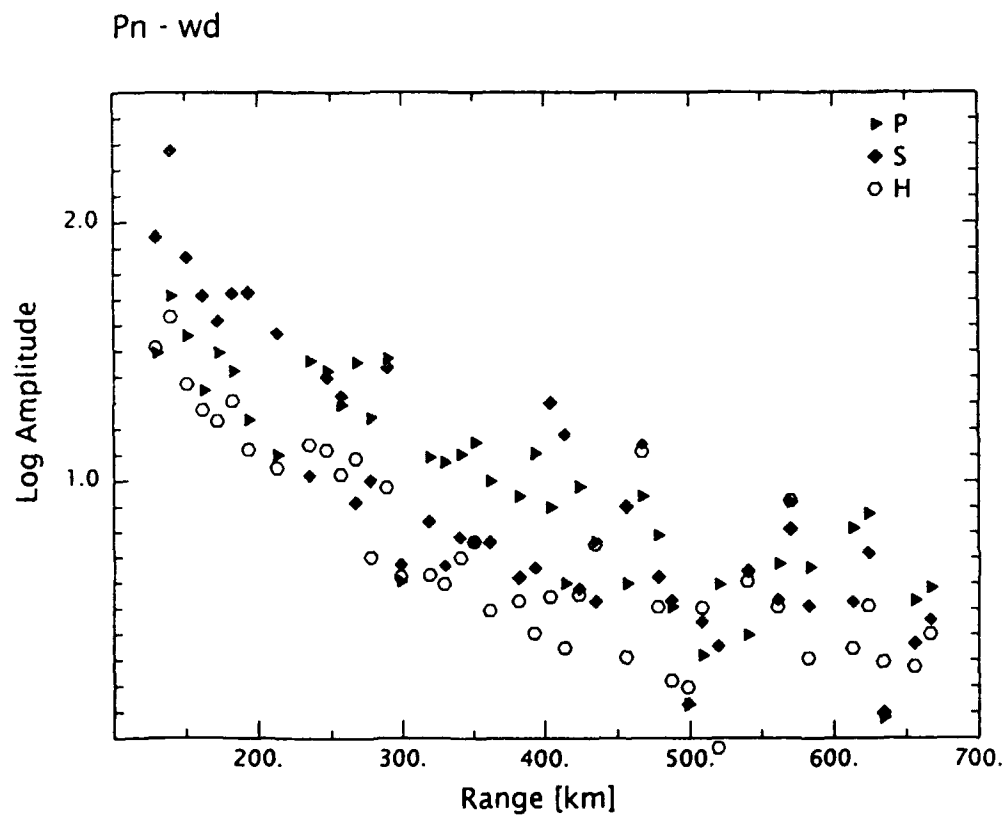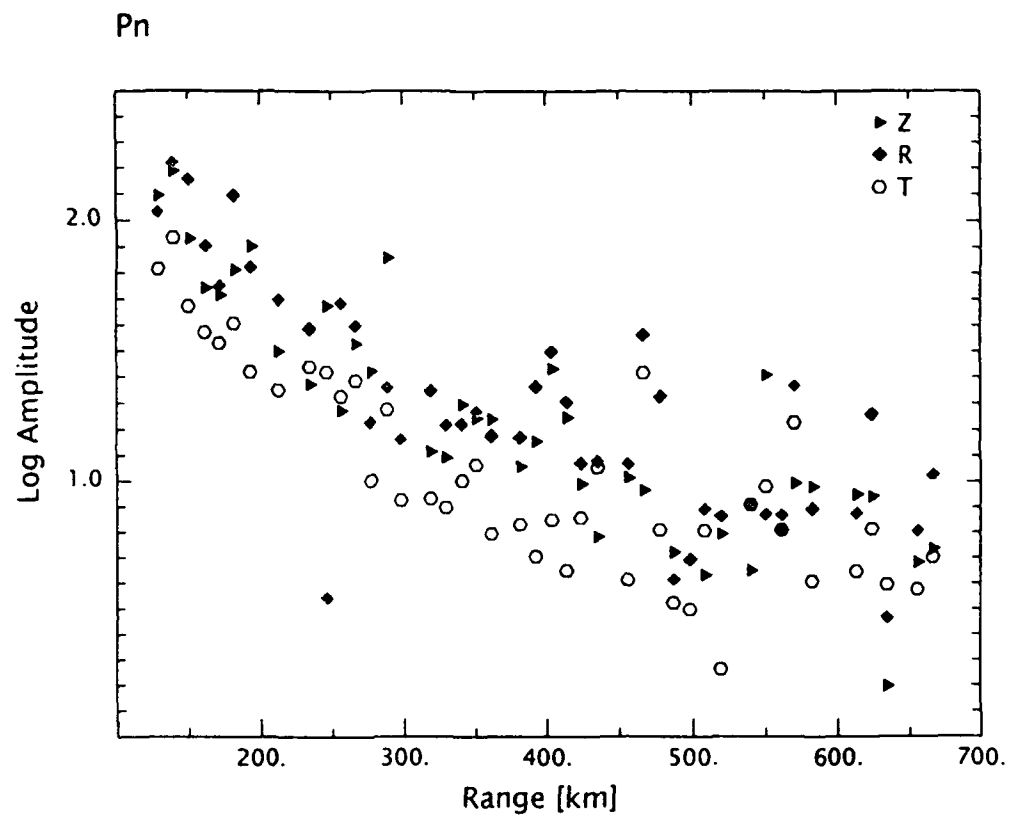
FIGURE 11

Sn

Sn - wd

FIGURE 12
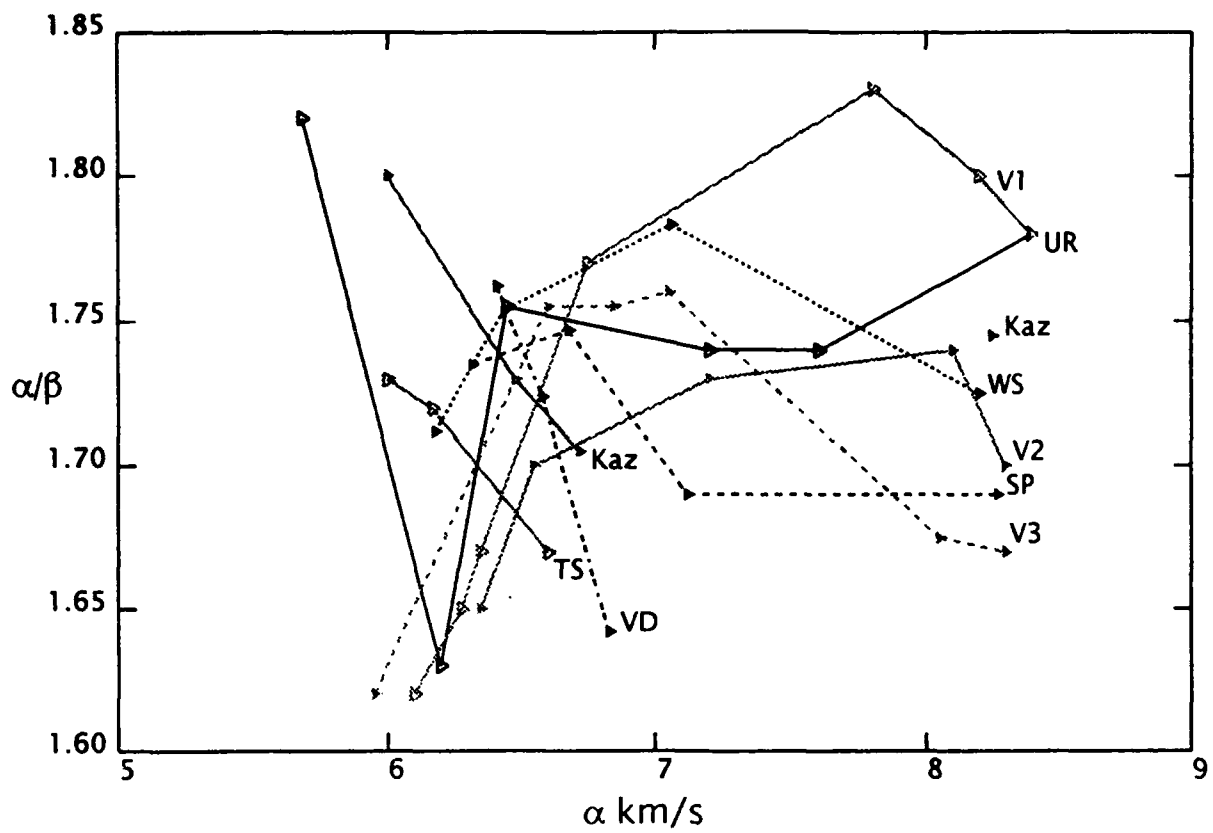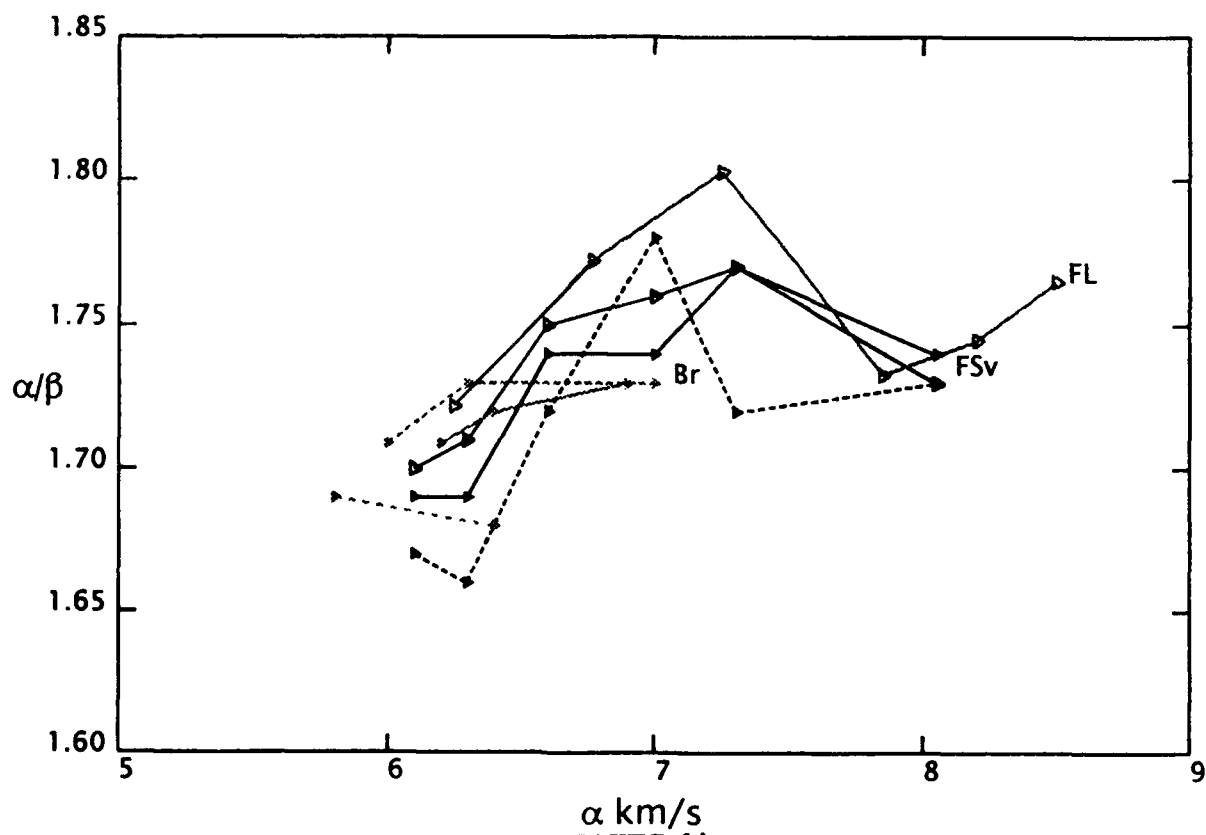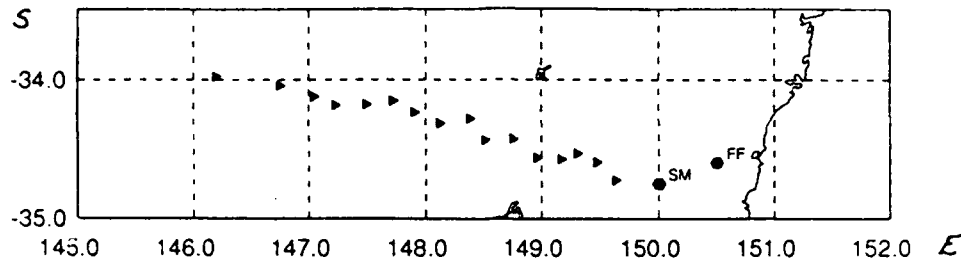
12

FIGURE 13

FIGURE 14

32

RAG 89/90

FIGURE 15

Fitzroy Falls
Earthquake

Distance [km]

FIGURE 16 (a)

15 traces

South Marulan
Quarry Blast

Distance [km]

FIGURE 16 (b)

15 traces

33
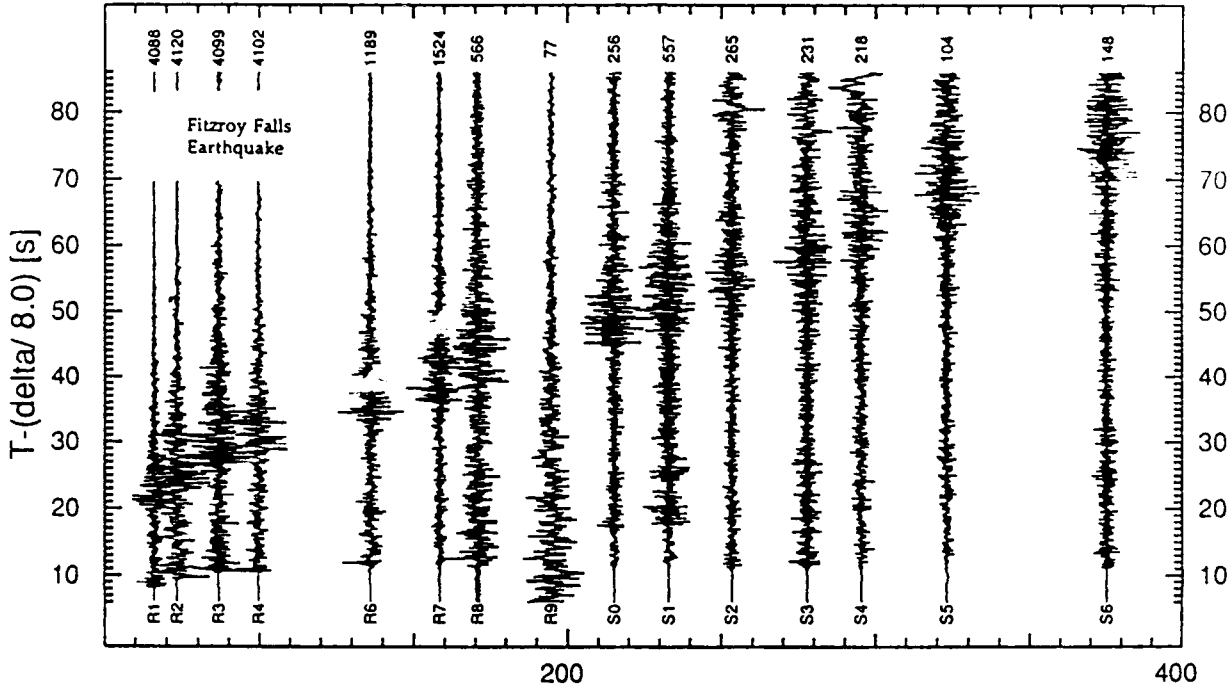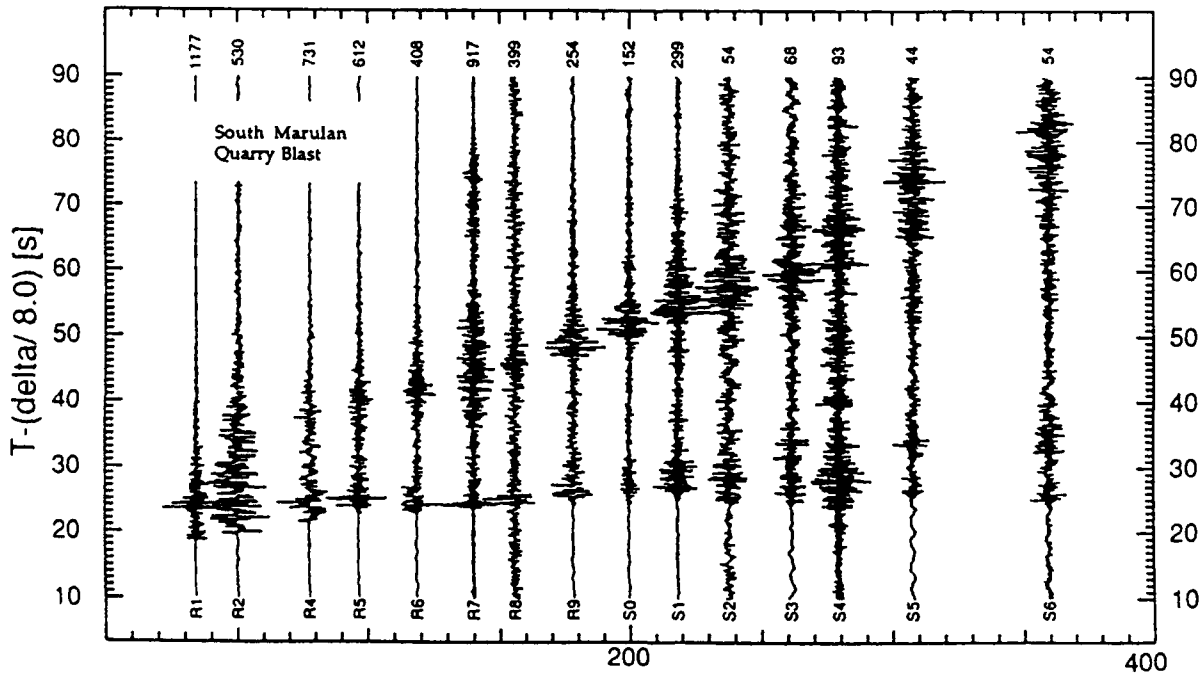
The distance dependence of regional phase discriminants .

B.L.N. Kennett
Research School of Earth Sciences, Australian National University,
G.P.O. Box 4, Canberra A.C.T. 2601, Australia

SUMMARY

Amplitude ratios of P and S phases recorded at regional distances have been suggested as potential discriminants for the character of seismic sources, because of the differences expected in the radiation patterns of earthquakes and well-contained explosions. The most useful reference phase for P waves beyond 200 km from the source is Pn and for S possible choices are the mantle phase Sn and the crustally guided wave Lg. Each of these phase has a different interaction with the seismic structure of the crust and mantle and such structural effects will impose their own patterns on the radiation characteristics from the source. The range dependent component in the Lg/Pn and Sn/Pn ratios have been investigated for a dense set of three-component records covering the distance range out to 700 km, for an explosive shot in water in southern Sweden which formed part of the 1979 Fennolora experiment. A stable measure of amplitudes and amplitude ratios is provided by using the vector resultant of ground motion (the square root of the total energy). However, even for a common source there are significant variations in the amplitude ratios for Lg/Pn and Sn/Pn of a factor of three or more as a function of range.

Keywords: Regional phases, three component records, Polarization, P-waves, S-waves, amplitude ratios, discrimination

Short title: Distance dependence of regional phase discriminants.

1. INTRODUCTION

The character of a seismic source imposes a distinctive radiation pattern on the seismic field which can then be modified by propagation phenomena such as conversion at the free surface or a major internal boundaries. A well-contained explosive source is expected to generate P waves directly and the accompanying S wave radiation observed at distance has to be produced by secondary action such as free-surface conversion. Whereas an earthquake source had an intrinsic shear component and should produce larger S than P wave energy. Measures of the relative amplitude of P and S wave are therefore attractive for discrimination between explosive and earthquake sources; and at regional distances are often implemented by using the ratios of the amplitudes of different P and S phases. The P and S phases which are being compared should have similar propagation characteristics, so that amplitude differences can be ascribed to the variation in the radiation at the source. The mantle phases Pn, Sn are expected to have similar propagation paths in the mantle but will sample only a relatively narrow angular range of radiation from the source. Since Pn is earliest arrival in the

distance zone from 200-1000 km it can normally be readily distinguished from background noise, but Sn has to be sought against the background of the P coda and its amplitude can be difficult to measure. The largest S phase out to 1000 km is usually the superposition of crustally guided S waves denoted by Lg in discrimination work. However Lg is known to be sensitive to variations in crustal structure and so is most effective as a reference for S waves when the propagation paths from different sources are very similar.

Amplitude ratios for the P and S phases are often computed on a component by component basis, but this procedure is susceptible to the influence of lateral heterogeneity in propagation. A more stable procedure is to use the vector amplitude of seismic displacement or its projection into a horizontal or vertical plane. The behaviour of such P/S amplitude ratios with distance from the source is investigated using record sections of three-component digital records from the Fennolora long range refraction profile in Sweden for an explosive source in shallow water.

VECTORIAL P/S AMPLITUDE RATIOS FOR REGIONAL PHASES

The Fennolora Project in Sweden in the summer of 1979 was a long-range refraction profile with three-component recording so that it is possible to study both the P and S components of the wavefield. In this study we use data from shot point B to the south of Sweden which has previously been used by Kennett (1993) to look at the propagation processes contributing to the character of the recorded regional phases. In figure 1, we display a record section for the radial component from 51 three-component sets of traces for the shot B3N at Fennolora shotpoint B, for distance ranges up to 675 km from the source. The traces have been filtered using a 4-pole Butterworth filter with 3 db points at 1 and 12 Hz. The trace amplitudes have been corrected for the scaling factors applied during the digitization of the original analogue records and so true amplitude relations are available between components. In the plotting a linear scale factor has been applied in range to emphasize the arrivals at greater ranges. The major phase groups (Pn, Sn and Lg) used in the subsequent analysis are indicated in figure 1.

Amplitude distribution with distance

For each of the main regional seismic phases we have extracted an amplitude distribution as a function of range by extracting the maximum amplitude found for a particular component or vector amplitude within a time window around the expected arrival time for the phase.

One representation of the vectorial pattern of ground motion is via the three orthogonal components vertical (Z) , radial (R) and tangential (T) which offer a convenient theoretical interpretation for stratified media with the separation of SH waves on the tangential component, and P-SV waves in a vertical plane defined by the vertical and radial components. This formulation is used as the basis of the approximate method of free-surface removal used by Kennett (1993) for the same Fennolora data, which is very effective in the display and analysis of the waveforms of the various phases.

However, a simpler alternative approach is to work directly with the vectorial character of the ground motion and to use vector resultants as a measure of the amplitude of the wavefield. We have used three different measures of the amplitude: the total vector resultant of motion,

$$t = [Z^2 + R^2 + T^2]^{1/2},$$

the vector amplitude in the vertical plane

$$v = [Z^2 + R^2]^{1/2},$$

and the vector amplitude projected into the horizontal plane

$$h = [R^2 + T^2]^{1/2}.$$

These three quantities can be easily constructed from the cartesian components of motion. Both the amplitude measures t and h are not dependent on the rotation of the horizontal components. For the Fennolora data the horizontal component seismometers were deployed in the radial and tangential directions but in general the azimuth to the source is not known so that there is an advantage in amplitude measures which do not require knowledge of azimuth. Booker & Mitronovas (1964) used a 3-component energy measure (t^2) on a study of a range of amplitude rations for explosions at the Nevada Test Site and a number of earthquakes observed using short-period Benioff instruments on the LRSM network.

Pn: The amplitude distributions for the Pn arrivals are displayed in figure 2 as a function of range. In the upper panel we show the amplitudes from the three cartesian components and in the lower panel the vector amplitude measures introduced above. For distances less than the crossover near 200 km there may be some influence from Pg but for larger ranges Pn is well separated from the other phases. The trends in the amplitude behaviour for Pn can be discerned in the cartesian components but a clearer in the vector representation. As would be expected for an explosive source in water most of the energy lies in the vertical plane but there is significant amplitude in the tangential component. The amplitude of Pn tends to decline with distance but there are some significant local increases which are likely to arise from changes in the near surface structure. There are also broader scale amplitude variations reflecting the complex substructure of the Pn phase arising from the influence of velocity variations in the lithosphere (see e.g. Fuchs & Schulz 1976).

Sn: As can be seen from figure 1, the emergence of the Sn phase from the Lg phase is less distinct than for the emergence of Pn and as a result the Lg energy dominates out to 300 km. As noted by Gajewski et al (1990) such behaviour is common on many refraction profiles, but profiles in Precambrian areas (see e.g Grad & Luosto 1987) can show strong Sn at the crossover with Sg. Beyond 300 km the amplitude patterns derived from the Fennolora data shown in figure 3 do reflect the Sn behaviour. There is a significant contribution from horizontal motion- indeed Kennett (1993) noted that a picking criterion for Sn could be based on an increase in energy in the horizontal plane. The vector measures of amplitude are again less scattered and show more systematic trends. There are indications of structure within the amplitude distribution but these are more

muted than for Pn. The Sn amplitudes are generally larger on the transverse component than the radial despite the fact that the source was an explosion in water. This arises, in part at least, from the fact that SH waves are amplified by a factor of two at the free surface whereas the amplification due to the interaction of the incident and reflected waves is less for SV because of interaction with the P wavefield.

Lg: We have already noted that the large amplitude Lg arrivals tend to swamp the smaller Sn phase out to 300 km. The phase is built up by a complex interference of multiple S reflections within the crust and as a result the maximum amplitude tends to shift relative to the asymptotic group velocity of close to 3.5 km/s as different contributions become important. The amplitude measures (both cartesian and vectorial) in figure 4 show a slow decline with distance, interrupted by some noise spikes, which could be modelled via an empirical attenuation function. The maximum amplitudes encountered at different distances can be associated with differing propagation processes and may not be suitable for direct comparison. However, when using a single seismogram the large amplitude Lg phase offers a convenient measure of the S field.

Amplitude ratios as a function of range
The amplitude distributions we have just discussed describe the behaviour of seismic phases whose propagation characteristics are quite complex and which display significant substructure. The influence of the differing trends in the amplitude behaviour becomes more pronounced when we take amplitude ratios between Sn and Lg and the reference Pn phase. We recall that we have a common explosive source in water for all the traces we have considered, so that the behaviour of the amplitude ratios with range reflects the influence of structure in the crust and upper mantle .

Sn/Pn ratio: We have used both the cartesian components and the vector amplitude measures to examine the distance dependance of the Sn/Pn ratio. As we have noted above the Sn amplitudes are contaminated by Lg for distances less than 300 km, but the time separation is sufficient for distinct Sn beyond 300 km. In the upper panel of figure 5 we display a component by component comparison of Sn/Pn amplitude ratios. There is some consistency in the behaviour for the vertical and radial component ratios, but the transverse components are not very useful because of the low amplitude of the tangential component for Pn. Even if the vertical component amplitudes for Pn are used as a reference there is still a large scatter in the behaviour of the tangential component for Sn. However if we make use of the vector measures of amplitude (shown in the lower panel of figure 5) the different amplitude ratios are much more consistent and a reasonably clear pattern emerges. The ratios of the total vector amplitude between Pn and Sn vary by a factor of 3 between 300 and 700 km as a result of the differences in the nature of the P and S structures in the upper mantle and the propagation paths for the particular phases.

Lg/Pn ratio: The amplitude ratios for the cartesian components are again rather chaotic as can be seen in the upper panel of figure 6. As for the Sn/Pn case part of the confusion arises from the small tangential component for Pn. The use of a constant reference to the vertical component of Pn generally reduces the scatter, but is not as useful as working directly with the ratios of the vector amplitude measures displayed in the lower panel of figure 6. A more consistent set of features can be found in this display but there are variations of at least a factor of four in the amplitude ratio for the same source over the distance range from 150 to 700 km. This arises because of the complex interplay between the influence of structure in the upper mantle on the Pn phase and the changing dominance of different orders of S wave crustal multiples for Lg.

3. DISCUSSION

The amplitude ratios presented in this paper are derived from a single source recorded along a profile where lateral variations in structure are modest (Stangl 1990). Nevertheless the ratios which are intended to provide a measure of the relative significance of the P and S show variations of a factor of three or more as a function of range. Although there are variations in the S phases much of the structure in the amplitude ratios with range comes from the way in which the reference phase Pn is built up from an en echelon set of sub-phases returned from the upper mantle (Kind 1974).

Amplitude ratios for P and S phases have a useful role to play as one class of discriminant in a decision making process based on the consensus of a wide range of different measures of source character, but we have to be cognizant of the likely influence of earth structure on their behaviour. Blandford (1980) has advocated the use of the ratio of the maximum amplitude for Pn and Lg on the vertical component. Our results suggest that a more stable amplitude ratio would be obtained by comparing vector amplitudes. The variation in the Lg/Pn ratios induced by structural effects may help to explain the considerable scatter in the Lg/P ratios observed by Mykkeltveit & Husbeye (1980) for earthquakes and explosions in Central Asia recorded in Norway. Lg is quite sensitive to crustal heterogeneity (see e.g. Bostock & Kennett 1990 and references therein), and this will tend to enhance the structural component in the Lg/Pn ratios for paths crossing major mountain chains or deep sedimentary basins. The Lg/Pn ratio can be a a potential discriminant for explosions and earthquakes in close proximity observed at a common set of stations but cannot be used indiscriminately. Sn is less sensitive to heterogeneity within the crust and for distances beyond 300 km the Sn/Pn ratio is likely to be a useful adjunct to other measures of source character.

The greater stability of the vectorial estimates of phase amplitude and consequently the P/S ratios is likely to arise because of the influence of three-dimensional structure during the propagation process. In a ray-based study of the effect of three-dimensional crustal structure on Lg waves, Bostock & Kennett (1990) have shown how the polarization of S waves will tend to tilt away from the initial vertical or horizontal planes as the wavefield encounters horizontal velocity gradients. As a result the recorded wavefield is likely to be best

represented by S wave groups whose polarization are not the simple SV and SH forms expected for a stratified medium. There will be similar tilting effects for the polarization of P waves which will no longer lie purely in a vertical plane. Under a rotation of the plane of rotation the amplitude of the vector disturbance associated with each wave type will be invariant and so vector amplitudes can be expected to have enhanced stability compared with amplitudes of individual components.

The total vector amplitude is readily constructed from any three-component record and does not require knowledge of the azimuth to the source (no prior rotation to radial and tangential components is required). The projection of the vector amplitude on a horizontal plane similarly just depends on the vector resultant of the two horizontal components. However, the vector amplitude in the vertical plane we have used does require the radial component and vertical components of motion.

REFERENCES

Blandford R.R. 1980, Seismic discrimination problems at regional distances, in *Identification of Seismic Sources - Earthquake or Underground Explosion*, eds Husebye E.S & Mykkeltveit S., 695-740, Riedel, Dordrecht.

Booker A. & Mitronovas W. 1964, An application of statistical discrimination to classify seismic events, *Bull. Seism. Soc . Am.*, **54**, 961-971

Bostock M.G. & Kennett B.L.N. 1990, The effect of 3-D structure on Lg propagation patterns, *Geophys. J. Int.*, **101**, 355-365.

Fuchs K. & Schulz K., 1976, Tunneling of low-frequency waves through the subcrustal lithosphere, *J. Geophys.*, **42**, 175-190.

Gajewski D., Stangl R., Fuchs K. & Sandmeier K.J., 1990, A new constraint on the composition of the topmost continental mantle - anomalously different depth increases of P and S velocity, *Geophys. J. Int.*, **103**, 497-507.

Grad M. & Luosto U., 1987, Seismic models of the crust of the Baltic shield along the SVEKA profile in Finland, *Annales Geophysicae*, **5B**, 639-650

Kennett B.L.N., 1993, On the nature of regional seismic phases - II . 3-component studies of crustal and mantle phases,*Geophys J. Int.*, submitted.

Kind R., 1974, Long range propagation of seismic energy in the lower lithosphere, *J. Geophys.*, **40**, 189-202.

Mykkeltveit S. & Husebye E.S. 1980, Lg wave propagation in Eurasia, in *Identification of Seismic Sources - Earthquake or Underground Explosion*, eds Husebye E.S & Mykkeltveit S., 421-451, Riedel, Dordrecht.

Stangl R., 1990, Die Struktur der Lithosphäre in Schweden, abgeleitet aus einer gemeinsamen Interpretation der P- und S-Wellen Registrierungen auf dem FENNOLORA-Profil, *Doktors der Naturwissenschaften Thesis*, University of Karlsruhe.

FIGURES:

Fig 1. Vertical component record section for seismometers across the southern part of Sweden, extracted from three-component data for the shots B3N at Fennolora shotpoint B. The seismograms are plotted with true amplitudes and a linear display gain in range.

Fig 2. The dependence of the maximum amplitude of the Pn phase as a function of range. Pn is separated from Pg beyond 200 km. The upper panel shows the cartesian components of motion and the lower a set of vector amplitude measures (t- total amplitude, v- amplitude in vertical plane, h- amplitude in horizontal plane).

Fig 3. The dependence of the maximum amplitude of the Sn phase as a function of range. Sn is not well separated from Lg until 300 km. The upper panel shows the cartesian components of motion and the lower a set of vector amplitude measures (t- total amplitude, v- amplitude in vertical plane, h- amplitude in horizontal plane).

Fig 4. The dependence of the maximum amplitude of the Lg phase as a function of range. The upper panel shows the cartesian components of motion and the lower a set of vector amplitude measures (t- total amplitude, v- amplitude in vertical plane, h- amplitude in horizontal plane).

Fig 5. The dependence of the amplitude ratio of Sn to Pn as a function of range. The upper panel presents the ratios of the cartesian components of motion and the lower the ratios of the vector amplitude measures

Fig 6. The dependence of the amplitude ratio of Lg to Pn as a function of range. The upper panel presents the ratios of the cartesian components of motion and the lower the ratios of the vector amplitude measures

RC - fennl obs

FIGURE 1

Range [km]

T - Range/8.0 [s]

42
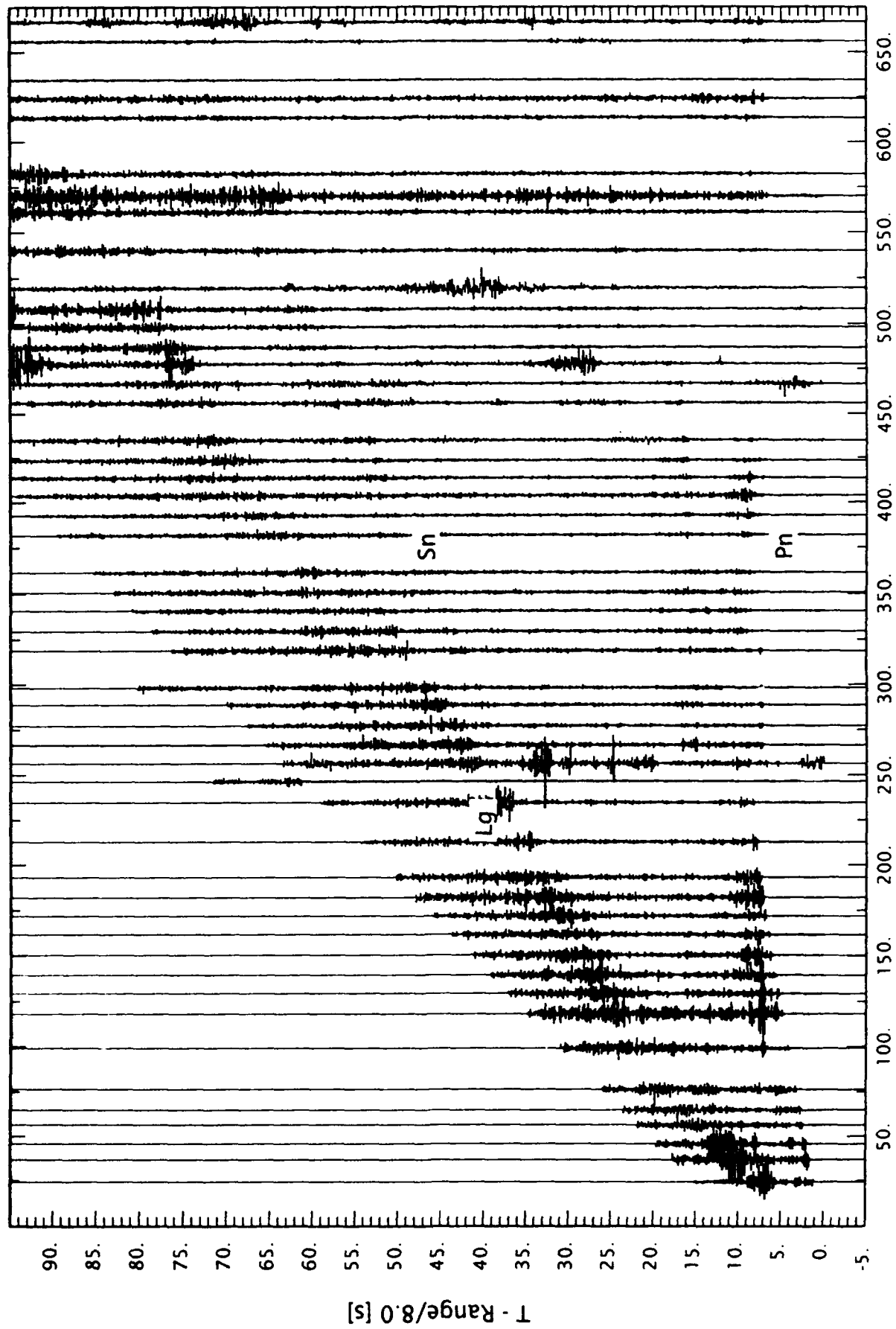
Pn
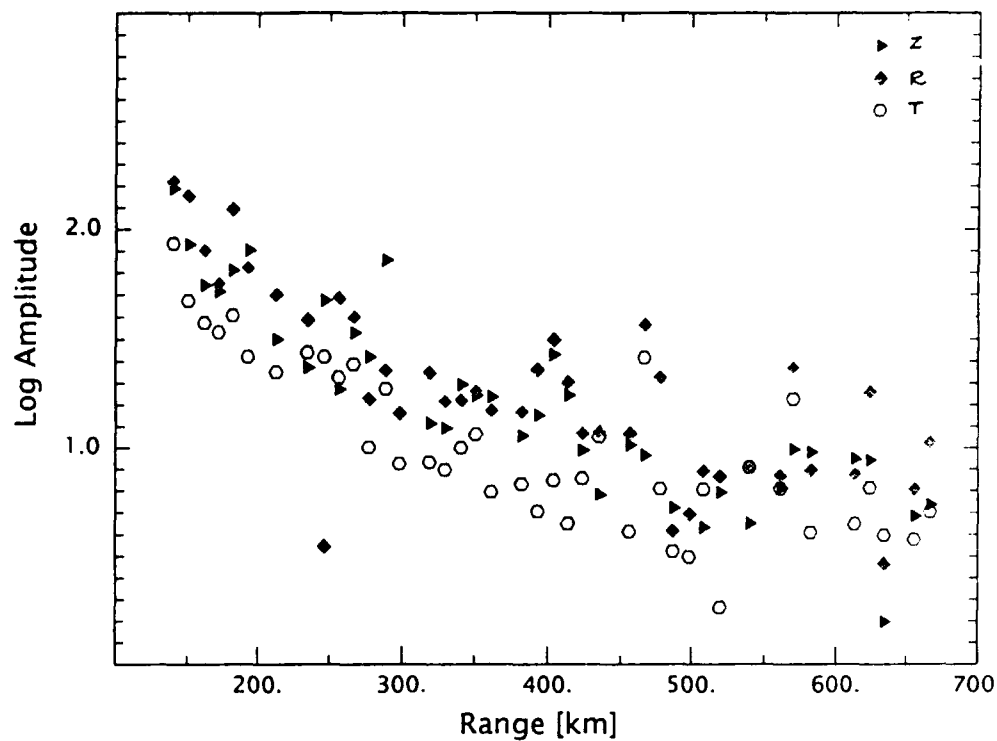
Pn vector amplitude
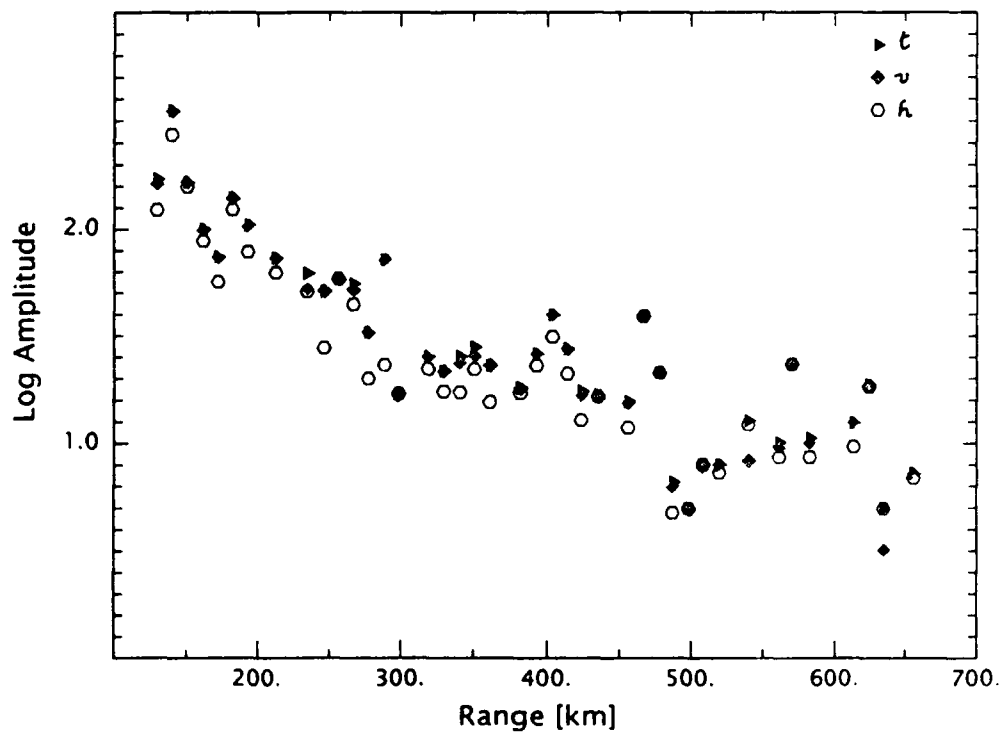
FIGURE 2
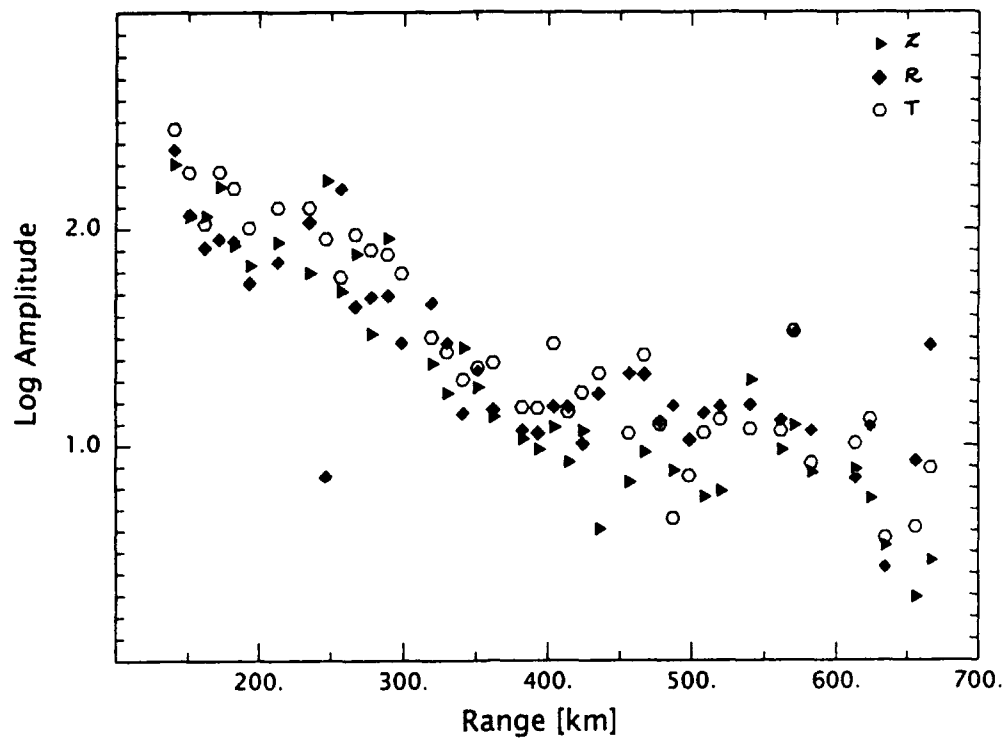
Sn vector amplitude
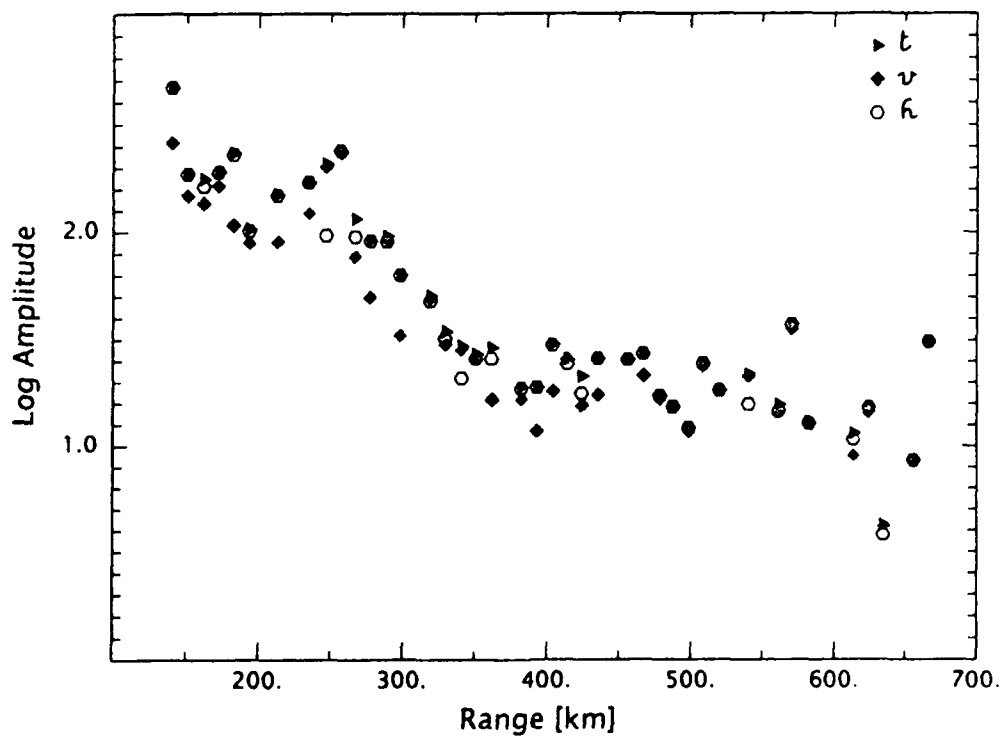
FIGURE 3

3

Lg
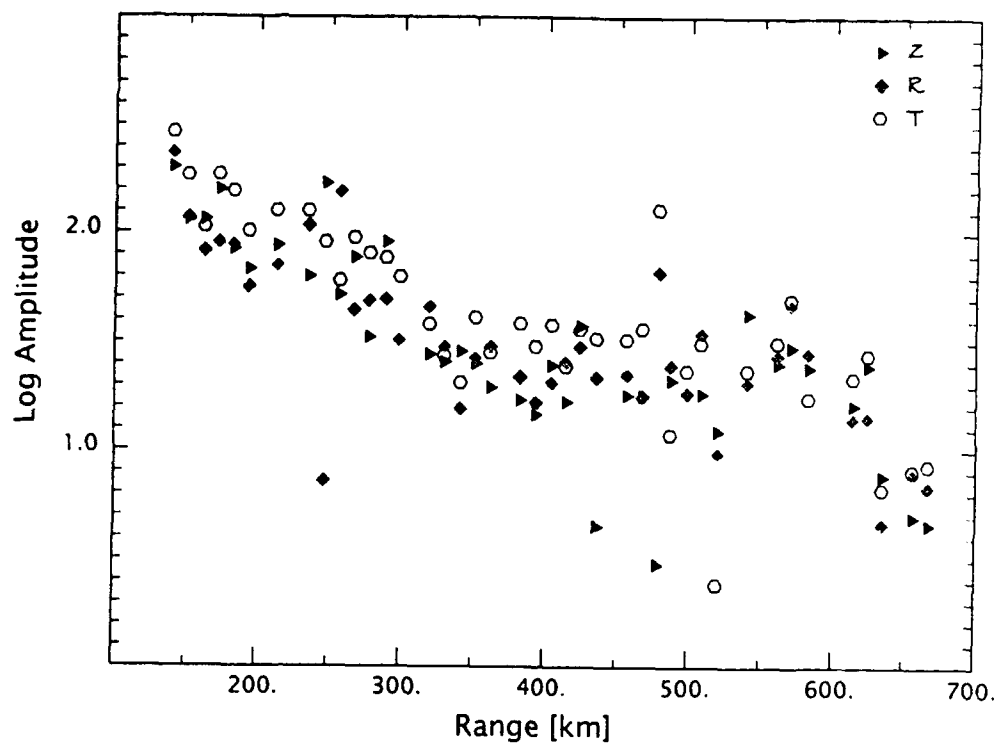
Lg   vector amplitude
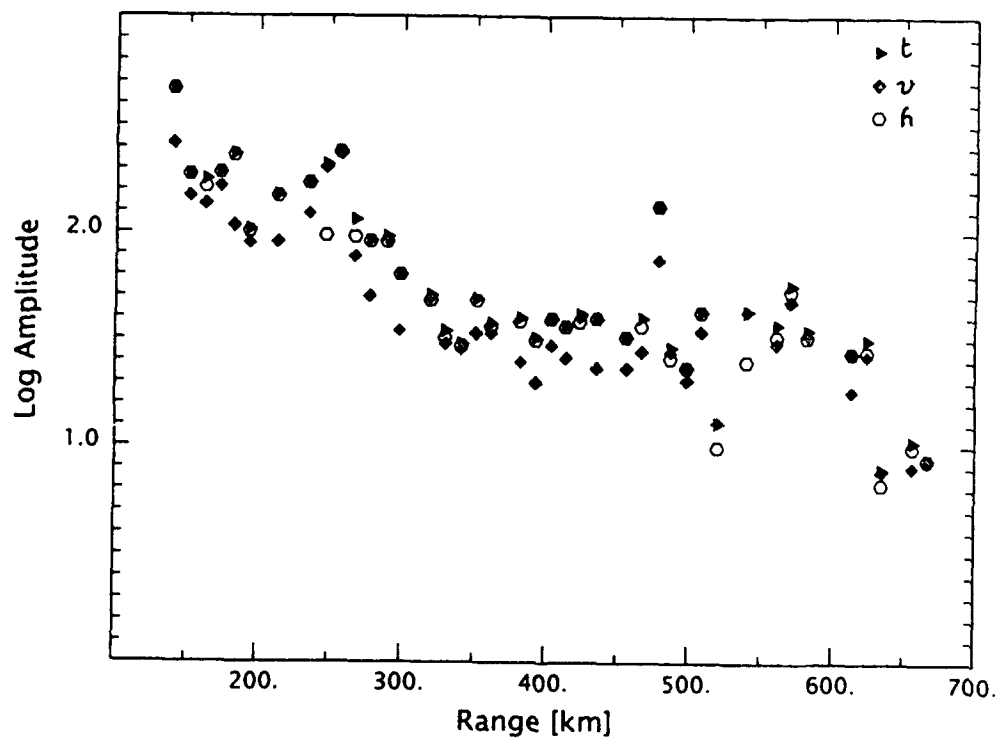
FIGURE 4
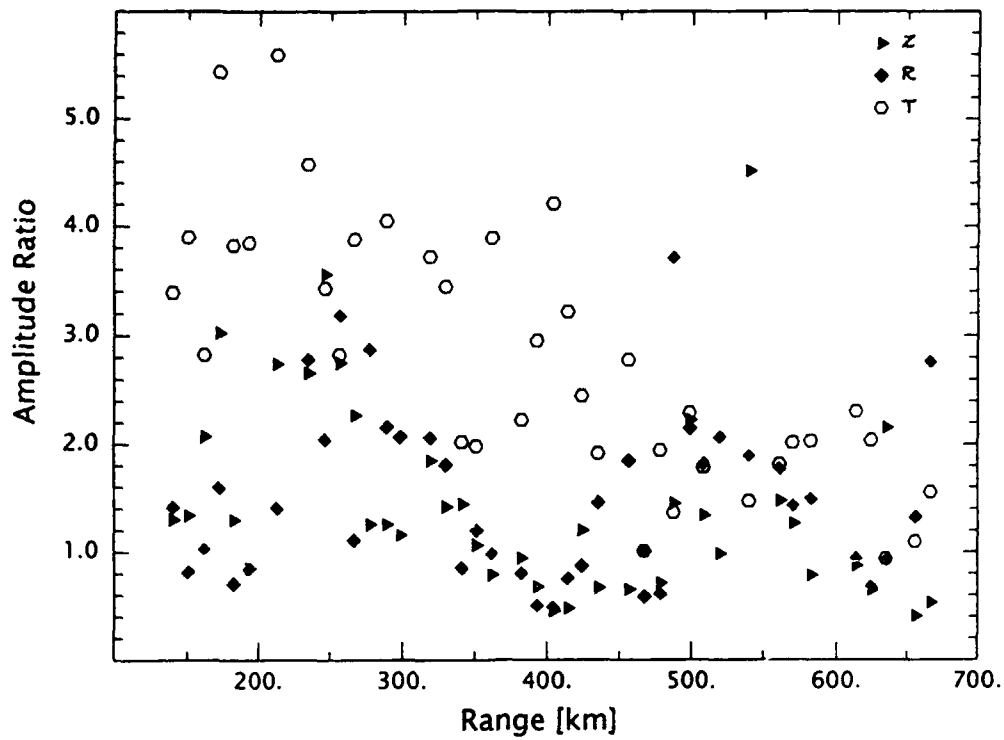
Sn/Pn Vector
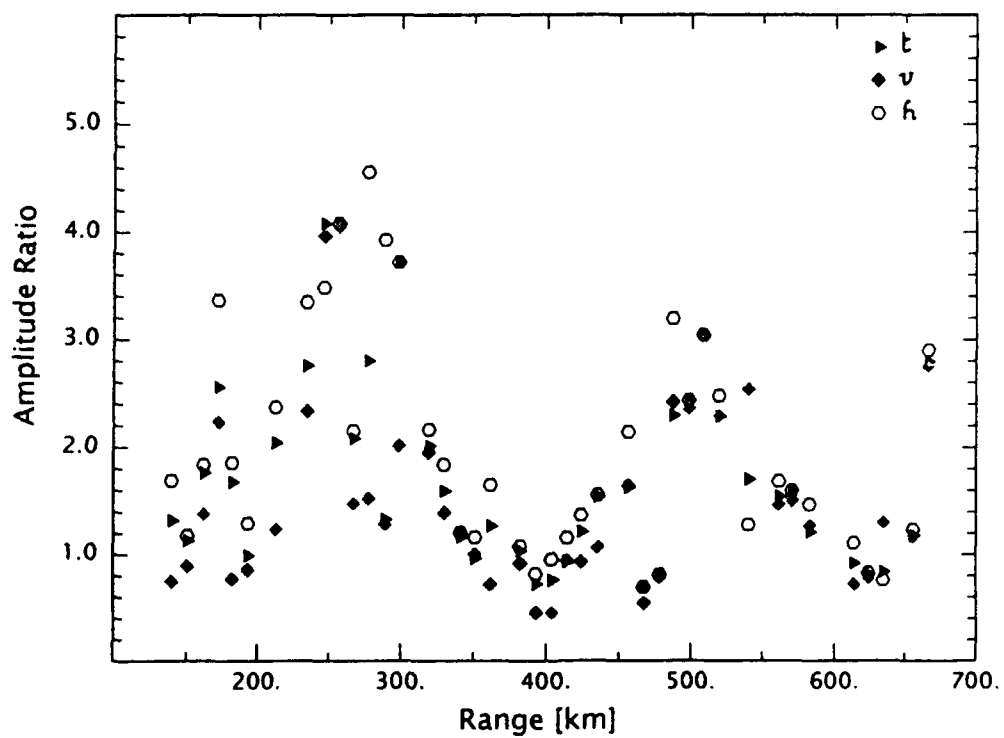
FIGURE 5

5
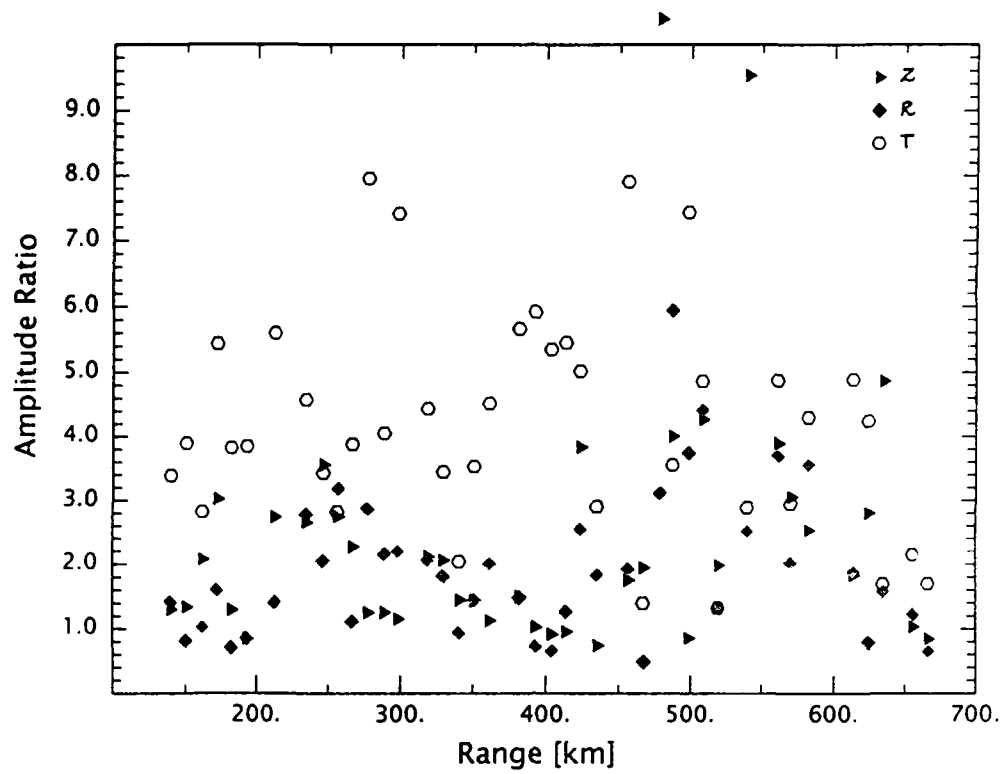
Lg/Pn

Lg/Pn - Vector

FIGURE 6

47
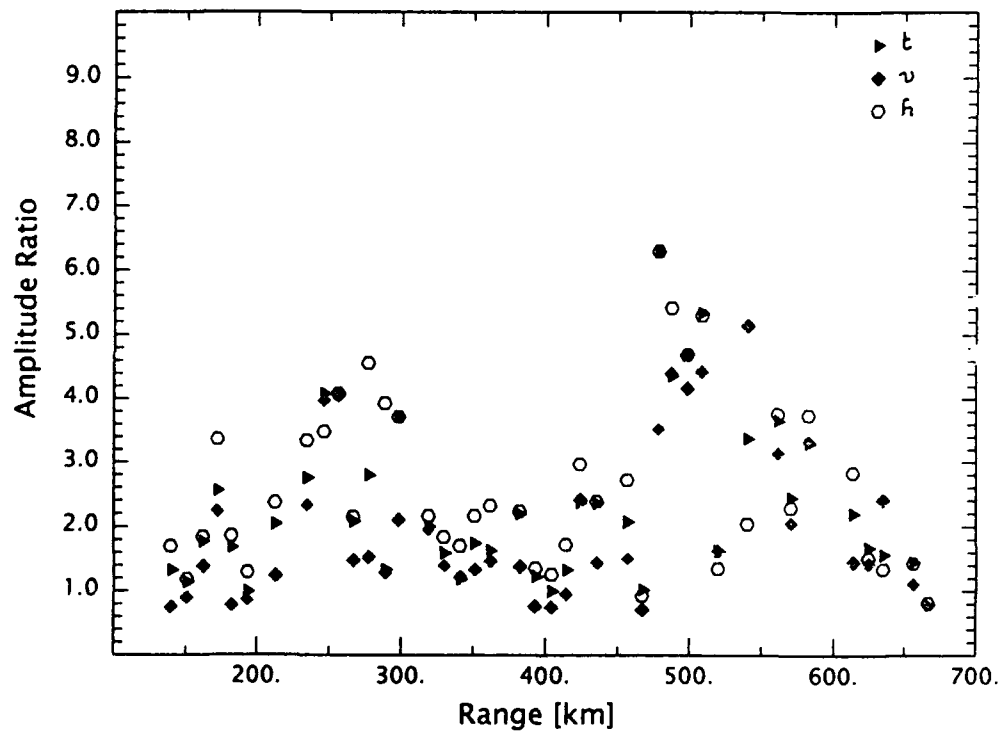
6.

Prof. Thomas Ahrens
Seismological Lab, 252-21
Division of Geological & Planetary Sciences
California Institute of Technology
Pasadena, CA 91125

Prof. Keiiti Aki
Center for Earth Sciences
University of Southern California
University Park
Los Angeles, CA 90089-0741

Prof. Shelton Alexander
Geosciences Department
403 Deike Building
The Pennsylvania State University
University Park, PA 16802

Dr. Ralph Alewine, III
DARPA/NMRO
3701 North Fairfax Drive
Arlington, VA 22203-1714

Prof. Charles B. Archambeau
CIRES
University of Colorado
Boulder, CO 80309

Dr. Thomas C. Bache, Jr.
Science Applications Int'l Corp.
10260 Campus Point Drive
San Diego, CA 92121 (2 copies)

Prof. Muawia Barazangi
Institute for the Study of the Continent
Cornell University
Ithaca, NY 14853

Dr. Jeff Barker
Department of Geological Sciences
State University of New York
 at Binghamton
Vestal, NY 13901

Dr. Douglas R. Baumgardt
ENSCO, Inc
5400 Port Royal Road
Springfield, VA 22151-2388

Dr. Susan Beck
Department of Geosciences
Building #77
University of Arizona
Tuscon, AZ 85721

Dr. T.J. Bennett
S-CUBED
A Division of Maxwell Laboratories
11800 Sunrise Valley Drive, Suite 1212
Reston, VA 22091

Dr. Robert Blandford
AFTAC/TT, Center for Seismic Studies
1300 North 17th Street
Suite 1450
Arlington, VA 22209-2308

Dr. Stephen Bratt
Center for Seismic Studies
1300 North 17th Street
Suite 1450
Arlington, VA 22209-2308

Dr. Lawrence Burdick
Woodward-Clyde Consultants
566 El Dorado Street
Pasadena, CA 91109-3245

Dr. Robert Burridge
Schlumberger-Doll Research Center
Old Quarry Road
Ridgefield, CT 06877

Dr. Jerry Carter
Center for Seismic Studies
1300 North 17th Street
Suite 1450
Arlington, VA 22209-2308

Dr. Eric Chael
Division 9241
Sandia Laboratory
Albuquerque, NM 87185

Dr. Martin Chapman
Department of Geological Sciences
Virginia Polytechnical Institute
21044 Derring Hall
Blacksburg, VA 24061

Prof. Vernon F. Cormier
Department of Geology & Geophysics
U-45, Room 207
University of Connecticut
Storrs, CT 06268

Prof. Steven Day
Department of Geological Sciences
San Diego State University
San Diego, CA 92182

Marvin Denny
U.S. Department of Energy
Office of Arms Control
Washington, DC 20585

Dr. Cliff Frolich
Institute of Geophysics
8701 North Mopac
Austin, TX 78759

Dr. Zoltan Der
ENSCO, Inc.
5400 Port Royal Road
Springfield, VA 22151-2388

Dr. Holly Given
IGPP, A-025
Scripps Institute of Oceanography
University of California, San Diego
La Jolla, CA 92093

Prof. Adam Dziewonski
Hoffman Laboratory, Harvard University
Dept. of Earth Atmos. & Planetary Sciences
20 Oxford Street
Cambridge, MA 02138

Dr. Jeffrey W. Given
SAIC
10260 Campus Point Drive
San Diego, CA 92121

Prof. John Ebel
Department of Geology & Geophysics
Boston College
Chestnut Hill, MA 02167

Dr. Dale Glover
Defense Intelligence Agency
ATTN: ODT-1B
Washington, DC 20301

Eric Fielding
SNEE Hall
INSTOC
Cornell University
Ithaca, NY 14853

Dr. Indra Gupta
Teledyne Geotech
314 Montgomery Street
Alexanderia, VA 22314

Dr. Mark D. Fisk
Mission Research Corporation
735 State Street
P.O. Drawer 719
Santa Barbara, CA 93102

Dan N. Hagedon
Pacific Northwest Laboratories
Battelle Boulevard
Richland, WA 99352

Prof Stanley Flatte
Applied Sciences Building
University of California, Santa Cruz
Santa Cruz, CA 95064

Dr. James Hannon
Lawrence Livermore National Laboratory
P.O. Box 808
L-205
Livermore, CA 94550

Dr. John Foley
NER-Geo Sciences
1100 Crown Colony Drive
Quincy, MA 02169

Dr. Roger Hansen
HQ AFTAC/TTR
Patrick AFB, FL 32925-6001

Prof. Donald Forsyth
Department of Geological Sciences
Brown University
Providence, RI 02912

Prof. David G. Harkrider
Seismological Laboratory
Division of Geological & Planetary Sciences
California Institute of Technology
Pasadena, CA 91125

Dr. Art Frankel
U.S. Geological Survey
922 National Center
Reston, VA 22092

Prof. Danny Harvey
CIRES
University of Colorado
Boulder, CO 80309

3

Dr. Gary McCartor
Department of Physics
Southern Methodist University
Dallas, TX 75275

Dr. Bao Nguyen
HQ AFTAC/TTR
Patrick AFB, FL 32925-6001

Prof. Thomas V. McEvilly
Seismographic Station
University of California
Berkeley, CA 94720

Prof. John A. Orcutt
IGPP, A-025
Scripps Institute of Oceanography
University of California, San Diego
La Jolla, CA 92093

Dr. Art McGarr
U.S. Geological Survey
Mail Stop 977
U.S. Geological Survey
Menlo Park, CA 94025

Prof. Jeffrey Park
Kline Geology Laboratory
P.O. Box 6666
New Haven, CT 06511-8130

Dr. Keith L. McLaughlin
S-CUBED
A Division of Maxwell Laboratory
P.O. Box 1620
La Jolla, CA 92038-1620

Dr. Howard Patton
Lawrence Livermore National Laboratory
L-025
P.O. Box 808
Livermore, CA 94550

Stephen Miller & Dr. Alexander Florence
SRI International
333 Ravenswood Avenue
Box AF 116
Menlo Park, CA 94025-3493

Dr. Frank Pilotte
HQ AFTAC/TT
Patrick AFB, FL 32925-6001

Prof. Bernard Minster
IGPP, A-025
Scripps Institute of Oceanography
University of California, San Diego
La Jolla, CA 92093

Dr. Jay J. Pulli
Radix Systems, Inc.
2 Taft Court, Suite 203
Rockville, MD 20850

Prof. Brian J. Mitchell
Department of Earth & Atmospheric Sciences
St. Louis University
St. Louis, MO 63156

Dr. Robert Reinke
ATTN: FCTVTD
Field Command
Defense Nuclear Agency
Kirtland AFB, NM 87115

Mr. Jack Murphy
S-CUBED
A Division of Maxwell Laboratory
11800 Sunrise Valley Drive, Suite 1212
Reston, VA 22091 (2 Copies)

Prof. Paul G. Richards
Lamont-Doherty Geological Observatory
 of Columbia University
Palisades, NY 10964

Dr. Keith K. Nakanishi
Lawrence Livermore National Laboratory
L-025
P.O. Box 808
Livermore, CA 94550

Mr. Wilmer Rivers
Teledyne Geotech
314 Montgomery Street
Alexandria, VA 22314

Dr. Carl Newton
Los Alamos National Laboratory
P.O. Box 1663
Mail Stop C335, Group ESS-3
Los Alamos, NM 87545

Dr. George Rothe
HQ AFTAC/TTR
Patrick AFB, FL 32925-6001

Prof. Clifford Thurber
University of Wisconsin-Madison
Department of Geology & Geophysics
1215 West Dayton Street
Madison, WS 53706

DARPA/PM
3701 North Fairfax Drive
Arlington, VA 22203-1714

Prof. M. Nafi Toksoz
Earth Resources Lab
Massachusetts Institute of Technology
42 Carleton Street
Cambridge, MA 02142

DARPA/RMO/RETRIEVAL
3701 North Fairfax Drive
Arlington, VA 22203-1714

Dr. Larry Turnbull
CIA-OSWR/NED
Washington, DC 20505

DARPA/RMO/SECURITY OFFICE
3701 North Fairfax Drive
Arlington, VA 22203-1714

Dr. Gregory van der Vink
IRIS, Inc.
1616 North Fort Myer Drive
Suite 1440
Arlington, VA 22209

HQ DNA
ATTN: Technical Library
Washington, DC 20305

Dr. Karl Veith
EG&G
5211 Auth Road
Suite 240
Suitland, MD 20746

Defense Intelligence Agency
Directorate for Scientific & Technical Intelligence
ATTN: DTIB
Washington, DC 20340-6158

Prof. Terry C. Wallace
Department of Geosciences
Building #77
University of Arizona
Tuscon, AZ 85721

Defense Technical Information Center
Cameron Station
Alexandria, VA 22314 (2 Copies)

Dr. Thomas Weaver
Los Alamos National Laboratory
P.O. Box 1663
Mail Stop C335
Los Alamos, NM 87545

TACTEC
Battelle Memorial Institute
505 King Avenue
Columbus, OH 43201 (Final Report)

Dr. William Wortman
Mission Research Corporation
8560 Cinderbed Road
Suite 700
Newington, VA 22122

Phillips Laboratory
ATTN: XPG
Hanscom AFB, MA 01731-5000

Prof. Francis T. Wu
Department of Geological Sciences
State University of New York
 at Binghamton
Vestal, NY 13901

Phillips Laboratory
ATTN: GPE
Hanscom AFB, MA 01731-5000

AFTAC/CA
(STINFO)
Patrick AFB, FL 32925-6001

Phillips Laboratory
ATTN: TSML
Hanscom AFB, MA 01731-5000

Phillips Laboratory
ATTN: SUL
Kirtland, NM 87117 (2 copies)

Dr. Michel Bouchon
I.R.I.G.M.-B.P. 68
38402 St. Martin D'Heres
Cedex, FRANCE

Dr. Michel Campillo
Observatoire de Grenoble
I.R.I.G.M.-B.P. 53
38041 Grenoble, FRANCE

Dr. Kin Yip Chun
Geophysics Division
Physics Department
University of Toronto
Ontario, CANADA

Prof. Hans-Peter Harjes
Institute for Geophysic
Ruhr University/Bochum
P.O. Box 102148
4630 Bochum 1, GERMANY

Prof. Eystein Husebye
NTNF/NORSAR
P.O. Box 51
N-2007 Kjeller, NORWAY

David Jepsen
Acting Head, Nuclear Monitoring Section
Bureau of Mineral Resources
Geology and Geophysics
G.P.O. Box 378, Canberra, AUSTRALIA

Ms. Eva Johannisson
Senior Research Officer
FOA
S-172 90 Sundbyberg, SWEDEN

Dr. Peter Marshall
Procurement Executive
Ministry of Defense
Blacknest, Brimpton
Reading FG7-FRS, UNITED KINGDOM

Dr. Bernard Massinon, Dr. Pierre Mechler
Societe Radiomana
27 rue Claude Bernard
75005 Paris, FRANCE (2 Copies)

Dr. Svein Mykkeltveit
NTNT/NORSAR
P.O. Box 51
N-2007 Kjeller, NORWAY (3 Copies)

Prof. Keith Priestley
University of Cambridge
Bullard Labs, Dept. of Earth Sciences
Madingley Rise, Madingley Road
Cambridge CB3 OEZ, ENGLAND

Dr. Jorg Schlittenhardt
Federal Institute for Geosciences & Nat'l Res.
Postfach 510153
D-3000 Hannover 51, GERMANY

Dr. Johannes Schweitzer
Institute of Geophysics
Ruhr University/Bochum
P.O. Box 1102148
4360 Bochum 1, GERMANY

7